Physics – Uspekhi **61** (8) 719 – 738 (2018)

REVIEWS OF TOPICAL PROBLEMS PACS numbers: 72.15.Gd, 73.43.Qt, **75.47. – m**, 75.47.Lx

Colossal magnetoresistance manganites

N G Bebenin, R I Zainullina, V V Ustinov

DOI: https://doi.org/10.3367/UFNe.2017.07.038180

Contents

Abstract. We review lattice, thermodynamic, transport, high-frequency, and optical properties of $Re_{1-x}D_xMnO_3$ manganites, where *Re* is a rare earth and *D* is usually an alkaline-earth element. Colossal magnetoresistance (CMR) is the most famous effect observed in manganites near the Curie temperature T_C. It is shown that the temperature and magnetic field dependences of the magnetocaloric effect, resistivity, magnetoresistance, Hall effect, and thermopower near T_C depend on whether the magnetic transition is of first or second order. The possibility of applying the well-known Banerjee criterion to inhomogeneous ferromagnets is discussed. Special attention is paid to various inhomogeneities characteristic of the manganites, including the coexistence of different crystallographic phases, metallic inclusions in the semiconductor matrix, and polarons.

Keywords: manganites, colossal magnetoresistance

1. Introduction

Studies of $Re_{1-x}D_xMnO_3$ manganites, where *Re* is a rare-earth element, and *D* is usually a bivalent element, started already in 1950 [1]. The theoretical comprehension of experimental results on the relationship between the metallic conductivity and ferromagnetic ordering led to the creation of the theory of double exchange [2–4]. Until the middle of the 1960s, the basic properties of manganites seemed to be explained quite satisfactorily (see, e.g., the review by Methfessel and Mattis in handbook [5]), and interest in these complex oxides died away.

A 'renaissance' came about 20 years ago, when an extremely large magnetoresistance of thin films of some lanthanum manganites was discovered near the Curie temperature T_C [6, 7]. This effect was called colossal magnetoresistance (CMR). To date, a great amount of experimental data has been published on the transport phenomena and lattice and optical properties of CMR materials, and a large number of models have been proposed for their interpretation. Special attention is paid to the theoretical and experimental study of phase separation in manganites [8–13]. In reviews [14–26], the results obtained are discussed from various standpoints.

The majority of the existing surveys concerning the properties of CMR materials were published ten or more years ago; in reviews published in recent years, either separate problems of the physics of manganites are considered or data are summarized that are related to a narrow class of compounds. The results obtained in the last decade have significantly broadened our knowledge about the properties of manganites and have made it necessary to reexamine some conclusions that seemed to be reliably established.

In this reviews, we discuss the lattice, thermodynamic, transport, high-frequency, and optical properties of manganites showing a CMR effect. Since this effect is observed near the transition from a ferromagnetic to a paramagnetic state, those manganites with an antiferromagnetic type of ordering are not considered here.

We believe that CMR materials can be considered heavily doped ferromagnetic semiconductors with a strong lattice and

N G Bebenin, R I Zainullina, V V Ustinov Mikheev Institute of Metal Physics, Ural Branch of the Russian Academy of Sciences, ul. S Kovalevskoi 18, 620108 Ekaterinburg, Russian Federation
E-mail: bebenin@imp.uran.ru

Received 15 June 2017, revised 14 July 2017
Uspekhi Fizicheskikh Nauk **188** (8) 801 – 820 (2018)
DOI: https://doi.org/10.3367/UFNr.2017.07.038180
Translated by S N Gorin; edited by A Radzig

magnetic disorder. The magnetic phase transition in them can be not only of the second, but also of the first order. Because of the presence of disorder, it is difficult to distinguish these two cases with the use of magnetic data alone; therefore, we analyze in detail the opportunity to apply the well-known Banerjee criterion in inhomogeneous ferromagnets. This part of the review, just as the examination of the magnetocaloric effect, is, we believe, of general physical interest.

Since the CMR effect is connected with the transition between the ferromagnetic and paramagnetic phases, we will discuss in detail the differences between manganites experiencing second- and first-order magnetic transitions.

A quantitative analysis of transport phenomena is possible only on the basis of data obtained on single-crystalline samples. It is also of fundamental importance to utilize the results of optical studies: without taking them into account, in our opinion, it is simply impossible to discuss such key problems of the physics of manganites as phase separation and the role of polarons.

The main focus of this review is on the lanthanum manganites $La_{1-x}Sr_xMnO_3$, $La_{1-x}Ba_xMnO_3$, and $La_{1-x}Ca_xMnO_3$, since only for these compounds is there a sufficiently complete set of experimental data. We, however, do not doubt that the basic regularities, especially observed in the vicinity of the magnetic transition, are identical in all CMR manganites. A discussion of the results of measurements is conducted on the phenomenological level, since, in our opinion, at present a consistent microscopic theory of the properties of manganites is absent.

The literature on CMR manganites is extremely large, and there is no opportunity to take into account all published data. For this reason, the bibliography does not pretend to be complete; in it, only those studies that were directly used by the authors in this review are indicated.

2. Specific features of manganite samples

In experimental work, polycrystalline and single-crystalline samples are, as a rule, used equally with thin films. The properties of thin films strongly depend on the method of preparation, utilized substrate, and thickness of the film; therefore, the data obtained on such samples will be discussed only in certain cases. Polycrystals are most frequently prepared by the method of solid-phase synthesis. The data on the crystal structure and magnetization are sufficiently reliable, but the temperature dependence of the resistivity of polycrystals depends substantially on the temperature of annealing [27] and is to a considerable degree determined by the size of crystallites [28]; therefore, for a study (at least a qualitative one) of the mechanisms of electron transfer, such samples are inapplicable.

Reliable data on the nature of transport phenomena in CMR manganites were obtained after developing the production methods of single crystals. They are usually grown by the floating-zone melting method with radiation heating, which is widely used for growing single crystals of oxides [29]. Brief information on the growth method of $La_{1-x}Sr_xMnO_3$ single crystals is given in Ref. [30]; detailed studies of the specific features of growing the different lanthanum manganites are published in Refs [31–34]. The single crystals grown have the shape of cylinders with a length on the order of 60–70 mm with a diameter of about 5 mm. As a rule, they are twinned.

The real composition of samples of manganites usually differs from the nominal composition. In the majority of cases, the oxygen content is not equal to 3. Since the radius of the O^{2-} ion is great (1.40 Å), the excess of oxygen does not mean the presence of oxygen in the interstitials, but rather the appearance of vacancies in the positions of La and Mn in approximately equal quantities [35, 36]. For example, the $LaMnO_{3+\delta}$ formula in reality implies $La_{1-\varepsilon}Mn_{1-\varepsilon}O_3$, where $\varepsilon = \delta/(3+\delta)$ [36]. Because even the production of $La_{1-x}D_xMnO_{3+\delta}$ polycrystals with $\delta = 0$ presents significant difficulties [37–39]; therefore, in the majority of cases, the magnitude of δ is in fact not controlled.

The composition of single-crystalline samples utilized in different experiments is more poorly controlled than the composition of polycrystals. First, during growth of single-crystals, manganese evaporates intensely; therefore, it is frequently necessary to add a small excess of this element to the charging feed. Second, the distribution coefficient $K = C_s/C_m$, where C_s and C_m are the concentrations of the bivalent element in the solid and liquid phases at the solidification front, can be substantially less than unity. The greatest value, $K = 0.9$, of the distribution coefficient was found in the case of the La–Sr manganites, and it weakly depends on the concentration of Sr and on other parameters. If D = Ba or Ca, then the distribution coefficient is noticeably less (0.7–0.8 if D = Ba, and 0.6–0.7 if D = Ca) and substantially depends on the concentration of Ba or Ca in the polycrystalline feedstock, on the gas pressure in the chamber, and on the crystal growth rate [31–33]. As a consequence, the distribution of the elements over the ingot in the case of $La_{1-x}Ba_xMnO_3$, and especially in the case of $La_{1-x}Ca_xMnO_3$, is strongly inhomogeneous. An attempt at a quantitative analysis of this distribution was made in Ref. [40]. Data about the oxygen content in manganite single crystals were not apparently published. There is reason to believe that the vacancies of oxygen are present in all single crystals of manganites studied to date.

3. Crystal structure

The crystal structure of CMR manganites is called perovskite, which is not completely correct. In the true (cubic) perovskite cell, which contains one formula unit, manganese ions would be located in the environment of six oxygen ions, which form a regular octahedron, and the angle of the Mn–O–Mn bond would be equal to 180°. In the lanthanum manganites, the perovskite structure is always somewhat distorted, since, first, the oxygen octahedra are rotated relative to each other and, second, the octahedra can undergo distortions as a result of the Jahn–Teller effect. An essential role is also played by the presence of vacancies, especially oxygen type ones. As a result, the lattice can be orthorhombic, can be rhombohedral, or (in rare cases) can belong to some other crystal system.

To describe the orthorhombic structure of manganites (Group No. 62 in the International Tables for Crystallography [41]), various settings can be involved, which differ in the choice of both the origin of coordinates and of coordinate axes. A detailed analysis of the symmetry elements and different settings that are encountered in the literature is given in the survey by Naish [42]. Further, we will consider the *Pnma* setting, since it is precisely this setting that is utilized in the International Tables [41]. The orthorhombic unit cell in this setting contains four formula units.

It was established in Ref. [43] that two orthorhombic phases can be realized in lanthanum manganites. The first of

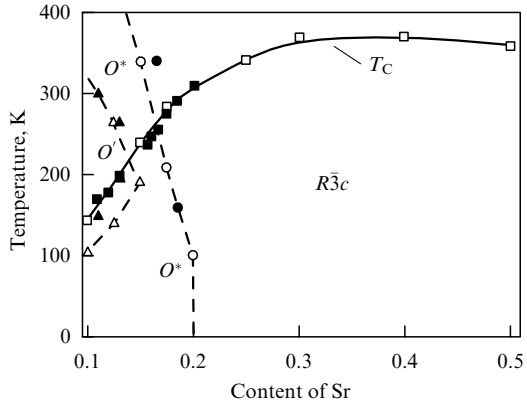

Figure 1. Phase diagram of the $La_{1-x}Sr_xMnO_3$ system. Filled symbols correspond to the data for polycrystals taken from Ref. [38]. Open symbols are the data for single crystals from Refs [30, 44].

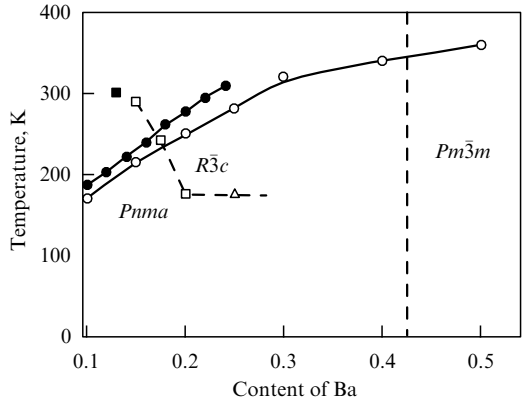

Figure 2. Phase diagram of the $La_{1-x}Ba_xMnO_3$ system. Solid symbols correspond to the data for the polycrystals taken from the work [37]. Open symbols are the data for single crystals from the studies [45, 49].

them (O'), with the lattice parameters $b/\sqrt{2} < c < a < b$, is characterized by strong Jahn–Teller distortions of oxygen octahedra. The second phase (O^*) is called pseudocubic. In this phase, the distortions of octahedra are weaker and $b/\sqrt{2} \sim c \sim a$; however, the Mn–O–Mn bond angles, just as in the O' phase, differ noticeably from 180°.

The rhombohedral lattice of manganites has the symmetry $R\bar{3}c$. The unit cell of this lattice is described by specifying the lattice parameter a and the angle α (see, e.g., Ref. [30]) or (more frequently) as a hexagonal unit cell. In the first case, the unit cell contains two formula units; in the second case, six formula units.

Figures 1–4 demonstrate the phase diagrams of La–Sr, La–Ba, and La–Ca manganites for compositions corresponding to the ferromagnetic ground state, i.e., for x from 0.1 to 0.5.

For $La_{1-x}Sr_xMnO_3$, data from Refs [30, 38, 44] have been borrowed: the filled symbols show the data for polycrystals, while the open symbols show the data for single crystals. The regions of existence of the phases are known sufficiently well; the transition temperatures determined from the experiments on polycrystals, which do not contain vacancies, and on single crystals barely differ.

In the case of $La_{1-x}Ba_xMnO_3$, the situation is different. The line dividing the regions of existence of the *Pnma* and $R\bar{3}c$ phases is known only partially, and the boundary between the rhombohedral $R\bar{3}c$ and cubic $Pm\bar{3}m$ phases, carried out according to Ref. [45], is very conditional, since it is based on measurements performed only at room temperature. According to Ref. [37], the large Jahn–Teller distortions of the oxygen octahedron at $T = 300$ K occur in the case of $x = 0.1$; at $x = 0.12$, these distortions are considerably weaker. Whether it is possible in this case to separate the regions of existence of the O' and O^* phases or not is unknown.

Notice that, according to Ref. [46], a transition from the rhombohedral to the monoclinic rather than to the orthorhombic phase occurs in a single crystal of $La_{0.815}Ba_{0.185}MnO_3$ at temperature $T = 187$ K. According to the authors of Refs [47, 48], in the polycrystalline $La_{0.7}Ba_{0.30}MnO_3$ the low-temperature orthorhombic phase has an *Imma* symmetry (Group No. 74), in which the distortions of octahedra are absent, and the *Imma* and $R\bar{3}c$ phases coexist in the temperature interval from 0 to at least 300 K [48].

The polycrystalline sample of $La_{1-x}Ba_xMnO_3$ with $x = 0.12$ was investigated at $T = 300$ K in Ref. [37]; it

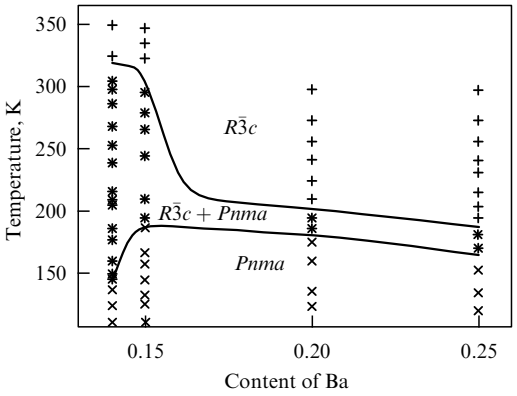

Figure 3. ($T-x$) phase diagram for the single crystals of $La_{1-x}Ba_xMnO_3$, in which the following crystalline phases are observed: (×) *Pnma*; (+) $R\bar{3}c$, or (∗) their mixture [49].

contains 97% orthorhombic phase and 3% rhombohedral phase, which indicates a noticeable 'smearing out' of the boundary between the *Pnma* and $R\bar{3}c$ phases, even in high-quality polycrystals. In Ref. [49], based on measurements of powders prepared by grinding single crystals, it was established that this smearing is a characteristic property of $La_{1-x}Ba_xMnO_3$. Figure 3 shows regions in which the *Pnma* and $R\bar{3}c$ phases were revealed. It can be seen that the width of the region of coexistence for $La_{0.75}Ba_{0.25}MnO_3$ and $La_{0.80}Ba_{0.20}MnO_3$ is on the order of 15–20 K, whereas at $x = 0.14$ and 0.15, the width of this region is on the order of 100 K.

Figure 4 depicts the phase diagram of $La_{1-x}Ca_xMnO_3$ constructed based on the data taken from Refs [50–53]. The rhombohedral phase exists at temperatures that exceed 700 K [50]; this part of the diagram will not be considered, since the CMR effect is observed at lower temperatures. The main area is occupied by the pseudocubic O^* phase; the Jahn–Teller phase O' exists only for $x < 0.2$. Although the symmetry of the lattice does not change upon a magnetic phase transition, a significant decrease (of about 0.13%) is observed in the $La_{0.75}Ca_{0.25}MnO_3$ volume upon the transition to the ferromagnetic phase [54]. According to Ref. [55], the relative change in the $La_{2/3}Ca_{1/3}MnO_3$ volume upon the magnetic transition is about 0.1%.

The physical properties of CMR materials strongly depend on the synthesis conditions, which determine the

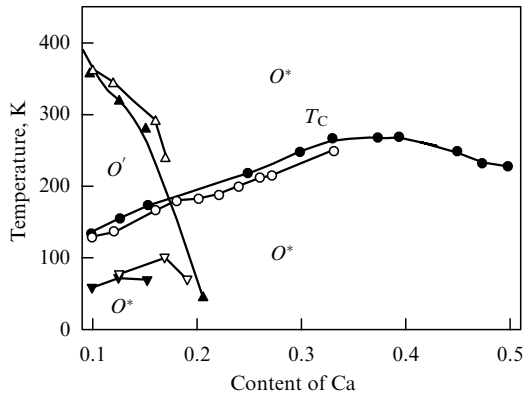

Figure 4. Phase diagram of the $La_{1-x}Ca_xMnO_3$ system. Filled symbols correspond to the data for polycrystals taken from Ref. [50]. Open symbols are the data for single crystals taken from Refs [51–53].

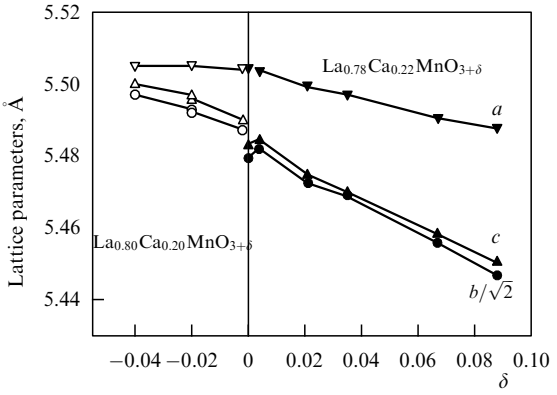

Figure 5. Dependences of the lattice parameters on the oxygen content. For $\delta < 0$, the data from Ref. [56] for the $La_{0.80}Ca_{0.20}MnO_{3+\delta}$ polycrystals are used; for positive δ, the data from Ref. [39] are taken.

stoichiometry of the samples obtained. As has already been noted, in the majority of cases the oxygen content differs from 3. A change in the oxygen content can lead to a change in the type of crystal structure. For example, the manganite of composition $La_{0.9}Ca_{0.1}MnO_{3+\delta}$ has an O' structure at room temperature if $\delta = 0$; a pseudocubic O^* structure if $\delta = 0.042$, 0.077, or 0.089, and a rhombohedral $R\bar{3}c$ structure if $\delta = 0.126$ and 0.159 [39]. Typical dependences of the parameters of the orthorhombic lattice on δ are illustrated in Fig. 5, where the data from Refs [39] and [56] are taken.

Upon substituting part of the lanthanum by strontium, barium, or calcium, the volume per formula unit decreases, and the Mn–O–Mn bond angle increases [37–39, 56, 57]. An increase in the pressure also leads to a decrease in the Mn–O bond lengths and an increase in the Mn–O–Mn bond angle [58, 59].

4. Thermodynamic characteristics of manganites

4.1 Structural transitions

The temperature of a first-order phase transition depends on external pressure P and magnetic field H. The Clapeyron equations have the following form

$$\frac{\partial T}{\partial P} = \frac{\Delta v}{\Delta S} = \frac{T\Delta v}{q}\,, \quad H = \text{const}\,, \tag{1}$$

$$\frac{\partial T}{\partial H} = \frac{-\Delta M(H)}{\Delta S} = \frac{-T\Delta M(H)}{q}\,, \quad P = \text{const}\,, \tag{2}$$

where Δv and $\Delta M(H)$ are the changes in the volume and in the magnetization upon the transition, ΔS is the change in the entropy, and q is the latent heat of the transition. In all manganites, the temperature of the transition from an orthorhombic (O) to a rhombohedral (R) phase depends on the pressure in a linear manner: $T_S(P) = T_S(0) + A^{(p)}P$, from which it follows that $\Delta S = q/T_S = (v^R - v^O)/A^{(p)}$. The heat of the transition can also be determined based on the change in T_S in a magnetic field. If $T_S < T_C$, then the change in the magnetization $\Delta M = M^R - M^O$ can be considered to be independent of the magnetic field strength, so that $T_S = T_S(0) + B_1H$, where the coefficient B_1 is given by the right-hand side of Eqn (2). If the structural transition occurs in the paramagnetic region, then $\Delta M(H) = \Delta\chi H$, where $\Delta\chi$ is the change in magnetic susceptibility; therefore, the shift of T_S upon changing the field from 0 to H is equal to B_2H^2, where $B_2 = -T_S(0)\,\Delta\chi/(2q)$.

Let us estimate the quantity q. Although many authors have mentioned the influence of pressure and magnetic field on the $Pnma - R\bar{3}c$ transition, the data on Δv and ΔM are scarce, to say nothing of $\Delta\chi$. For the $La_{1-x}Sr_xMnO_3$ single crystals, the necessary information is given in Refs [60, 61]. The values of Δv lie between 0.1 and 0.2 Å^3/Mn; the magnitude of $A^{(p)}$ is equal to 5–7 K kbar^{-1}. The obtained values of the heat of the transition are on the order of 0.1–0.2 kJ mol^{-1}. The values of q determined from data on the shift of the transition temperature in a magnetic field are close to those obtained from data on the pressure dependences.

In $La_{1-x}Ba_xMnO_3$, the change in the volume of the unit cell upon the $Pnma - R\bar{3}c$ transition is on the order of 0.01 – 0.02 Å^3 [49] and, in fact, lies within the limits of the experimental error; therefore, for q we can perform only a plausible estimation. For an $La_{0.8}Ba_{0.2}MnO_3$ single crystal, an $A = -3$ K bar^{-1} value was found in papers [62, 63], so that $q = 0.04 - 0.08$ kJ mol^{-1}. On the other hand, $B_1 = -0.45 \times 10^{-4}$ K Oe^{-1}, $\Delta M = 4$ G [62, 64], from which we find $q = 0.06$ kJ mol^{-1} that is in agreement with the estimate obtained from the data on the $T_S(P)$ dependence.

The latent heat of the structural transition in the manganites in question is very small; moreover, in the case of lanthanum–barium crystals, the magnitude of q is a fraction of that in the lanthanum–strontium manganites. Possibly, it is precisely for this reason that the width of the structural transition in $La_{1-x}Ba_xMnO_3$ is noticeably greater than the analogues magnitude in $La_{1-x}Sr_xMnO_3$.

4.2 Ferromagnetic–paramagnetic transition

Temperature T_C of the transition from the ferromagnetic to the paramagnetic state in $La_{1-x}D_xMnO_3$ manganites depends nonlinearly on the concentration of the bivalent ion (see Figs 1, 2, 4). In the case of $La_{1-x}Sr_xMnO_3$, the Curie temperatures found for polycrystalline and single-crystalline samples practically coincide. If D = Ba, Ca, then the values of T_C for single crystals lie below the values for the polycrystals, which, apparently, indicates a noticeably larger defectiveness in the La–Ba and La–Ca single crystals.

In all lanthanum manganites, the Curie temperature rises upon applying pressure (see, e.g., Refs [65–67]).

In $La_{1-x}Sr_xMnO_3$ and $La_{1-x}Ba_xMnO_3$ manganites, the magnetic transition proceeds as a second-order phase transition. In $La_{1-x}Ca_xMnO_3$, the situation is different: the transition from the ferromagnetic to paramagnetic state is a second-order phase transition if $x < 0.25$, whereas at higher concentrations of calcium this transition acquires signs of the first-order phase transition. In other words, it is possible to consider that in the phase diagram of $La_{1-x}Ca_xMnO_3$, the concentration $x_{tr} = 0.25$ corresponds to a tri-critical point (see paper [53] and references cited therein).

Since a first-order magnetic transition is observed in $La_{0.7}Ca_{0.3}MnO_3$, and a second-order transition takes place in $La_{0.7}Sr_{0.3}MnO_3$, it can be expected that there is some $La_{0.7}Ca_{0.3-y}Sr_yMnO_3$ composition in which a value of y will correspond to a tri-critical point. It was shown in Ref. [68] that the value $y = 0.1$ corresponds to this point.

As has already been indicated, a characteristic property of manganite single crystals is a nonuniform distribution of elements over the ingot. Since the Curie temperature strongly depends on composition, especially at small x, the Curie temperature proves to be a random function of coordinates, which leads to 'smearing out' the transition. Let us consider how this smearing can be characterized in the case of a second-order phase transition.

Let us assume that in the region with a local Curie temperature $\tau_C(\mathbf{r})$ the local value of the magnetization $\mu(\mathbf{r})$ satisfies the equation of the Landau theory:

$$H = A\mu + B\mu^3 , \tag{3}$$

where H is the magnetic field, $A(\mathbf{r}) = a[T - \tau_C(\mathbf{r})]$, and a and B are constants. Let μ^* be a solution to the equation

$$H = \langle A\rangle\mu^* + B\mu^{*3} , \tag{4}$$

where $\langle A\rangle = a(T - T_C)$. Here, the angular brackets $\langle ...\rangle$ mean averaging over the sample, and $T_C = \langle\tau_C\rangle$. In the experiment, it is in fact T_C or a quantity close to it that is determined. Expanding $\mu(A)$ into a series over the powers of $\delta A = A - \langle A\rangle$, namely

$$\mu(A) = \mu^* + \frac{d\mu^*}{d\langle A\rangle}\,\delta A + \frac{1}{2!}\,\frac{d^2\mu^*}{d\langle A\rangle^2}\,(\delta A)^2 + \dots ,$$

after the calculation of derivatives and averaging, we obtain the following expression for the experimental value of the average magnetization $M = \langle\mu\rangle$:

$$M = \mu^* + \frac{\langle A\rangle\,\mu^*\langle(\delta A)^2\rangle}{(A + 3B\mu^{*2})^3} . \tag{5}$$

Assuming δA to be small, let us replace μ^* by M on the right-hand part of Eqn (5) and substitute the result into Eqn (4) to obtain

$$\frac{H}{M} = \langle A\rangle + BM^2 - \frac{\langle A\rangle^3}{\left(\langle A\rangle + 3BM^2\right)^2}\,\frac{\sigma_{\tau_C}^2}{(T_C - T)^2} . \tag{6}$$

Here, $\sigma_{\tau_C} = \langle(\tau_C - T_C)^2\rangle$ is the standard deviation of the Curie temperature. If the demagnetizing factor N is different from zero, the field H in Eqns (3)–(6) can be considered to be the internal field $(H - 4\pi NM)$.

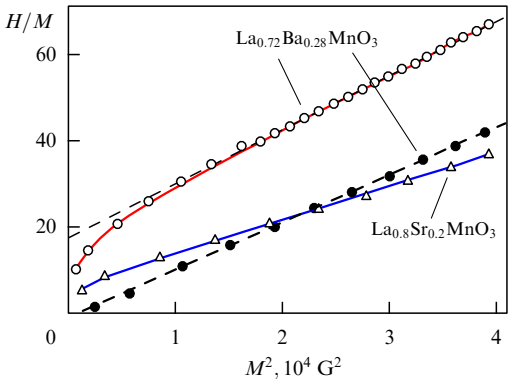

Figure 6. Belov–Arrott curves for single crystals of $La_{0.72}Ba_{0.28}MnO_3$ (open circles, $T = 315$ K; filled circles, $T = T_C = 311$ K) and $La_{0.8}Sr_{0.2}MnO_3$ (open triangles, $T = 307$ K) taken from Ref. [40]. Solid lines are calculations according to equation (6); dashed line is the linear approximation.

The equation obtained is equivalent to the one that was derived many years ago by Shtrikman and Wohlfarth [69]. If the smearing-out of the transition is absent ($\sigma_{\tau_C} = 0$), then equation (6) is reduced to the usual equation that is applied in the method of thermodynamic coefficients for determining the Curie temperature (Belov–Arrott curves). But, if $\sigma_{\tau_C} \neq 0$, this coincidence takes place only at $T = T_C$, since in this case the last term in equation (6) becomes zero. The conditions for the applicability of formula (6) are obvious: the magnetization M must be small in comparison with the saturation magnetization, and the last term on the right-hand side of formula (6) must be less than the sum of the first two terms.

Let us examine what the application of equation (6) gives for the investigation of the inhomogeneous magnetic state of manganite single crystals. Figure 6 shows Belov–Arrott curves for $La_{0.72}Ba_{0.28}MnO_3$ and $La_{0.8}Sr_{0.2}MnO_3$ single crystals, taken from Ref. [40]. In the case of $La_{0.72}Ba_{0.28}MnO_3$, the value of H/M is directly proportional to M^2 at a temperature of 311 K; therefore, $T_C = 311$ K. The use of equation (6) gives $\sigma_{\tau_C} \approx 3.2$ K. For the lanthanum–strontium manganite, $T_C = 306$ K, and $\sigma_{\tau_C} \approx 0.8$ K. As in the case of the *Pnma*–$R\bar{3}c$ structural transition, the magnetic inhomogeneity of the lanthanum–strontium crystal proves to be noticeably less than in the case of the lanthanum–barium crystal.

If the magnetic transition is referred to a first-order one, a jump in magnetization must be observed at the Curie temperature. In a magnetic field, T_C is displaced toward higher temperatures, $T_C(H) = T_C(0) + B_M H$, and the magnitude of the jump decreases. In a certain critical field H_{crit}, the jump in magnetization becomes zero, and for $H > H_{crit}$ the temperature dependence of the magnetization becomes smooth. Consequently, in the $(T-H)$ plane, we have $T = T_{crit} \equiv T_C(H_{crit})$ at the critical point and $H = H_{crit}$ is the endpoint of the line of phase transitions (critical point). Such a behavior was observed in a study of the $Sm_{0.55}Sr_{0.45}MnO_3$ [70] and $Sm_{0.52}Sr_{0.48}MnO_3$ polycrystals [71]. For $H < 40$ kOe, a jump in the magnetization is observed, and magnetic and temperature hystereses take place, whereas for $H > 40$ kOe the temperature dependence of the magnetization becomes smooth, similar to the $M(T)$ dependence in the vicinity of a second-order phase transition. Since at $H = 40$ kOe the maximum of the heat capacity was revealed at a temperature of approximately 160 K, it can be concluded that in these manganites $H_{crit} = 40$ kOe and

$T_{crit} = 160$ K. In other manganites, no such behavior, apparently, was observed, which can be connected with the high value of the critical field.

Because of the inhomogeneity of the manganites, a more or less smooth change in the magnetization is observed in the $M(T, H = \text{const})$ curve, instead of a jump. The use of the method of thermodynamic coefficients in this case leads to incomprehensible results. For example, the authors of Ref. [72], who investigated $La_{1-x}Ca_xMnO_3$ polycrystals, plotted a curve of the dependence of H/M on M^2 and used the Banerjee criterion [73], which follows from the Landau theory: if the sign of the derivative $\partial(H/M)/\partial(M^2)$ is positive, the transition is of the second order; if the sign is negative, the transition is of the first order. It turns out that for manganites with $x = 0.25$ and 0.275 the slope of these curves is always positive; however, their appearance differs significantly from that typical of the second-order transitions (see inset to Fig. 7). The authors of paper [72] believe that in such cases it is impossible to speak at all about the type of phase transition (therefore, they designated the temperature that corresponds to the point of inflection in the $M(T)$ curve as T_f rather than as T_C).

In our opinion, this conclusion is too categorical, and it is possible to speak of the type of transition, but it is necessary to refine the range of applicability of the Banerjee criterion in the case of inhomogeneous ferromagnets. For our purposes, it is reasonable to formulate this criterion as follows: if an inequality

$$\frac{\partial M}{\partial H} - \frac{M}{H} > 0 \qquad (7)$$

is fulfilled, a first-order phase transition is observed; if the reverse inequality is fulfilled, the transition is of the second order.

Let us consider a ferromagnet undergoing the first-order phase transition. At $H = 0$, the magnetization experiences a jump at the transition point from $M = M_f$ to zero. Assume that the values of the local Curie temperatures τ_C at $H = 0$ lie in the range from $T_{C1}(0)$ to $T_{C2}(0)$. If the width of the transition region is small, $\delta T_C = T_{C2}(0) - T_{C1}(0) \ll T_{C1}$, then the application of a magnetic field leads to shifts of T_{C1} and T_{C2} toward larger temperatures with an identical rate. Let us assume that the temperature T of the sample lies between $T_{C1}(0)$ and $T_{C2}(0)$ both in a zero magnetic field and for $H \neq 0$. If the magnetic field is sufficiently weak, it can be assumed that the change in the magnetization at a selected temperature is connected only with the shift of the transition region in the magnetic field. In this case, the magnetization of the sample is proportional to the volume of the ferromagnetic phase:

$$M(T, H) = M_f \int_{T - B_M H}^{T_{C2}(0)} W(\tau_C)\, d\tau_C\,, \qquad (8)$$

where W is the distribution function of the Curie temperatures. Let us assume for simplicity that a uniform (rectangular) distribution is realized: $W = (\delta T_C)^{-1}$ if $T_{C1}(0) < \tau_C < T_{C2}(0)$, and $W = 0$ outside this interval. Then, the average value of the Curie temperature is equal to $T_C = (T_{C2} + T_{C1})/2$, and the magnetization $m = M/M_f = [T_{C2}(0) - T + B_M H]/\delta T_C$, so that

$$\frac{\partial M}{\partial H} - \frac{M}{H} = -\frac{(T_{C2} - T)\, M_f}{H \delta T_C} < 0\,.$$

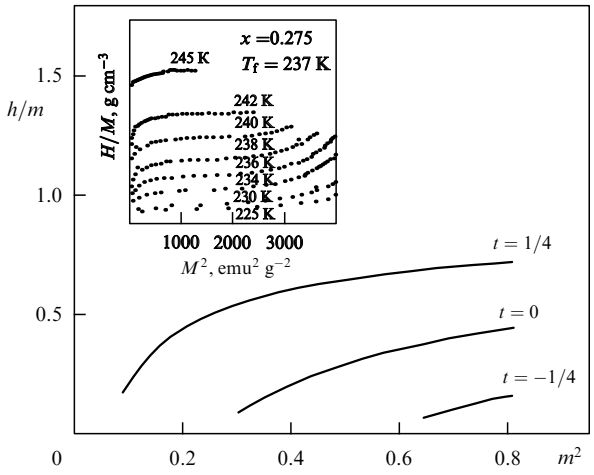

Figure 7. Belov–Arrott curves in the case of smeared-out first-order magnetic transition (calculation). In the inset: dependence of H/M on M^2 for the $La_{0.725}Ca_{0.275}MnO_3$ polycrystal, taken from Ref. [72].

We see that the Banerjee criterion indicates the second rather than the first order of the transition, i.e., the application of this criterion leads to the incorrect conclusion about the type of a phase transition.

Figure 7 shows the ratio h/m (where $h = B_M H/\delta T_C$) as a function of m^2 for three values of $t = (T - T_C)/\delta T_C$. It may be seen that the theoretical curves have the same shape as the experimental curves at small values of magnetization: $M^2 < 2000$ emu^2 g^{-2} (emu is the electromagnetic unit).

A similar result is obtained with the use of a Gaussian distribution function [74]. Since in this case the local Curie temperature falls into the interval $[T_C - \sigma_{\tau_C}, T_C + \sigma_{\tau_C}]$ with a probability of 0.68, into the interval with a width of two standard deviations from T_C with a probability of 0.95, and into the interval with a width of three standard deviations with a probability of 0.997, it is possible to put T_{C2} equal to $T_C + 2\sigma_{\tau_C}$ or $T_C + 3\sigma_{\tau_C}$.

Outside the transition region, the smearing-out effect of the transition is weak and is described by equation (6). It can turn out, however, that for $T > T_{C2}$ the magnetization of the sample grows almost linearly with an increase in the field value, which makes it impossible to determine the type of a phase transition from magnetic data.

Earlier, we assumed that the shape of the distribution function was given. It follows from formula (8) that the shape of W can be found from the temperature dependence of the magnetization in a weak field, since

$$\frac{\partial M(T, H = 0)}{\partial T} = -M_f W(T)\,.$$

An analysis performed in Ref. [74] showed that for single-crystalline $La_{0.7}Ca_{0.3}MnO_3$ the coefficient $B_M = 0.8$ K kOe^{-1}, $T_C(0) = 227$ K, $M_f = 343$ G, and the distribution function can be considered to be Gaussian with a standard deviation $\sigma_{\tau_C} = 7$ K. In the $La_{0.7-x}Pr_xCa_{0.3}MnO_3$ single crystals, the distribution function has a more complex asymmetrical form; therefore, average Curie temperature T_C is not equal to temperature T_M, which corresponds to the point of inflection in the curve of the temperature dependence of the magnetization [74].

The magnetic inhomogeneity of single crystals of lanthanum manganites depends on the type of the bivalent ion. The

smallest standard deviation σ_{τ_C} of the Curie temperature was found in the $La_{1-x}Sr_xMnO_3$ single crystals; in $La_{1-x}Ca_xMnO_3$, the value of σ_{τ_C} is largest. Many authors interpret the disorder in manganites as a consequence of the difference between the ionic radii of lanthanum and other ions in the A position of the perovskite unit cell, using for the quantitative estimation the quantity $s^2 = \sum y_i r_i^2 - \langle r_A \rangle^2$, where y_i is the fraction of the ith ion with a radius r_i, and $\langle r_A \rangle$ is the average value of the ionic radius. The ionic radii of lanthanum, calcium, strontium, and barium are equal to 1.36, 1.34, 1.44, and 1.61 Å, respectively [75]. It can easily be shown that at a given x the value of s^2 is smallest for La–Ca crystals and is greatest for La–Ba crystals, which contradicts the above estimations.

The single crystals of manganites are usually grown by the floating-zone melting method. The uniformity of the samples depends in this case on the distribution coefficient $K = C_s/C_m$, where C_s and C_m are the concentrations of the element A in the solid and liquid phases, respectively. Indeed, the distribution coefficient for strontium is close to unity (≈ 0.9); for barium, it is noticeably less ($\approx 0.7-0.8$), and for calcium, $K \approx 0.6$–0.7 (see Refs [31, 33]).

In the case of polycrystals, the width of the magnetic transition region substantially depends on the specific features of the synthesis processes.

Since the phase transition from the ferromagnetic to paramagnetic state in the $La_{0.7}Ca_{0.3}MnO_3$ manganite is a first-order one, it is possible to determine the latent heat of transition for it. Taking into account the results of Refs [54, 55], we will assume that the relative change in the volume in La–Ca manganites at a calcium content close to 0.3 is $\approx 0.1\%$, so that $\Delta v = 0.06$ Å^3/Mn $= 0.036$ cm^3 mol^{-1}. For the polycrystalline $La_{0.67}Ca_{0.33}MnO_3$, it was found by Neumeier et al. [67] that $\partial T_C/\partial P = 16$ K GPa^{-1}, from which we obtain an estimate $q = 0.49$ kJ mol^{-1}. The magnitude of q can also be calculated from magnetic data. As noted above, for a single crystal of $La_{0.7}Ca_{0.3}MnO_3$, the derivative $\partial T_C/\partial H = 0.8$ K kOe^{-1}, and the jump in the magnetization upon transition is $M_f = 343$ G. With the aid of equation (2), we find $\Delta S = 1.5$ J mol K$^{-1} = 7.1$ J kg^{-1} K^{-1}, so that $q = 0.34$ kJ mol^{-1}. The latent heat of the magnetic transition in $La_{1-x}Ca_xMnO_3$ at x close to 0.3 is several times greater than the value of q for the structural transition $Pnma - R\bar{3}c$ in the La–Sr and La–Ba manganites, although the magnitude of Δv is noticeably less. It is quite probable that the large magnitude of q in La–Ca manganites is due to magnetostriction.

Both the structural and magnetic transitions manifest themselves well in the temperature dependence of the thermal expansion $\Delta l/l$. In the case of $La_{2/3}Ca_{1/3}MnO_3$, a sharp peak is observed at $T = T_C$, whereas the observed feature is very weak in the curve for $La_{2/3}Sr_{1/3}MnO_3$ [76]. This difference is apparently caused by the fact that in $La_{2/3}Ca_{1/3}MnO_3$ a magnetic first-order transition occurs, and in $La_{2/3}Sr_{1/3}MnO_3$ the transition is of the second order.

In the transition region from the ferromagnetic to the paramagnetic state, and also in the region of structural transitions, a strong dependence of $\Delta l/l$ on the magnetic field is observed (see, e.g., Refs [77, 78]).

4.3 Magnetocaloric effect

Near a phase transition, the change in the entropy in a magnetic field, $\Delta S = S(H) - S(0)$, reaches large values [79, 80]. The magnetocaloric effect (MCE) was experimentally studied mainly in polycrystalline samples of manganites; work with the involvement of single crystals is scarce. A survey of data obtained before 2007 can be found in Ref. [81]. Since the interest in the magnetocaloric effect is mainly due to the prospects for its use in magnetic refrigerators, the connections between the MCE and other properties of manganites usually draw little attention. Below, some results are given concerned with the inhomogeneities inherent in lanthanum manganites.

We begin with materials in which the magnetic transition runs as the second-order process. In the case of an inhomogeneous ferromagnet, the following expression for $\Delta S(H)$ can be obtained within the framework of the Landau theory:

$$\Delta S(H) = -\frac{a}{2}\left[\langle \mu^2(H)\rangle - \langle \mu^2(0)\rangle\right]. \tag{9}$$

In Ref. [82], it was noted that this expression can be employed for finding the characteristics of the smearing-out of the phase transition. Assume that $T = T_C$. In this case, in a sufficiently strong magnetic field, we have $M = (H_{int}/B)^{1/3}$, where H_{int} is the internal field. In order to calculate $\langle \mu^2(0)\rangle$, we should know the distribution function W. The authors of Ref. [82] used a uniform distribution; in our opinion, a normal (Gaussian) distribution is more realistic. After calculating $\langle \mu^2(0)\rangle$, we obtain [83]

$$\Delta S(H) = -\frac{a}{2}\left[\left(\frac{H}{B}\right)^{2/3} - \frac{8\pi N}{3B} - \frac{a\sigma_{\tau_C}}{\sqrt{2\pi}B}\right]. \tag{10}$$

We retained here only the term that is linear in the standard deviation σ_{τ_C}. It was shown in Ref. [83] that the value of σ_{τ_C} determined with the aid of expression (10) for single crystals of $La_{0.72}Ba_{0.28}MnO_3$ ($\sigma_{\tau_C} = 2.7$ K) is close to the value ($\sigma_{\tau_C} = 3.2$ K) found from the analysis of Belov–Arrott curves.

If the magnetic transition is of a first order, then the $\Delta S(H)$ dependence proves to be substantially different. Let us first calculate ΔS in the vicinity of an ideally sharp first-order transition, when $M = \mu$ and $T_C = \tau_C$; in addition, we assume that the demagnetizing factor N is equal to zero. The change in the entropy is defined by the Clapeyron equation (2). In weak magnetic fields, the Curie temperature linearly depends on the magnetic field strength: $T_C(H) = T_C(0) + B_M H$, and the dependence of $\Delta M = M_p - M_f$ on H can be ignored (M_p is the magnetization of the paramagnetic phase). Since in weak fields we have $M_p \ll M_f$, it can be assumed that $M(T, H) = M_f\theta[T_C(0) + B_M H - T]$ and that $(\partial M/\partial T)_H = -M_f\delta[T_C(0) + B_M H - T]$. Using the well-known relationship

$$\Delta S(H) = \int_0^H \left(\frac{\partial M}{\partial T}\right)_H \mathrm{d}H, \tag{11}$$

we find that $\Delta S = 0$ for $T < T_C(0)$, and $\Delta S = -(M_f/B_M)$ for $T > T_C(0)$ and $H > (T - T_C(0))/B_M$.

If $N \neq 0$, then the situation becomes more complex. In this case, the uniform ferromagnetic phase exists for $T < T_C(0) + B_M(H - 4\pi N M_f)$, whereas the uniform paramagnetic phase exists for $T > T_C(0) + B_M H$. Inside the interval $T_C(0) + B_M(H - 4\pi N M_f) < T < T_C(0) + B_M H$, therefore, the uniform magnetic state is not realized; the ferromagnetic and paramagnetic phases coexist in the temperature interval with the width $\delta_N = 4\pi N M_f B_M$.

Using the data given for a single crystal of $La_{0.7}Ca_{0.3}MnO_3$, it can easily be shown that the real width of the magnetic transition region is an order of magnitude

greater than δ_N; therefore, the co-existence of the ferromagnetic and paramagnetic phases revealed in Refs [12, 13] is almost completely caused by the distribution of the Curie temperatures inside the crystal. Assuming that the distribution function W is Gaussian, we obtain in this case with the aid of relationships (8) and (11) [83]:

$$\Delta S(T,H) = -\frac{M_\mathrm{f}}{2B_\mathrm{M}}\left[\mathrm{erf}\left(\frac{x_0}{\sqrt{2}}\right) - \mathrm{erf}\left(\frac{x_H}{\sqrt{2}}\right)\right], \qquad (12)$$

where

$$x_0 = \frac{T - T_\mathrm{C}(0)}{\sigma_{\tau_\mathrm{C}}}, \quad x_H = \frac{T - T_C(0) - B_\mathrm{M}(H - 4\pi\bar{M}N)}{\sigma_{\tau_\mathrm{C}}},$$

and $\bar{M}$ is determined from the equality $T - T_\mathrm{C}(0) - B_\mathrm{M}(H - 4\pi N\bar{M}) = 0$. As was shown in Ref. [83], the $\Delta S(T, H = \mathrm{const})$ curves calculated via equation (12) agree well with the experimental data for a single crystal of $La_{0.7}Ca_{0.3}MnO_3$.

A simple analysis of Eqn (12) shows that, if $N = 0$, the maximum of the function $|\Delta S(T, H = \mathrm{const})|$ with an increase in the magnetic field is displaced toward higher temperatures at a rate of $B_\mathrm{M}/2$, and the maximum value of this function grows with an increase in the strength of the magnetic field:

$$|\Delta S|_\mathrm{max} = \frac{M_\mathrm{f} H}{\sqrt{2\pi}\sigma_{\tau_\mathrm{C}}}.$$

A shift of the point of the maximum is observed in all known cases; however, the rate of this displacement is not yet published. In the $La_{0.7}Ca_{0.3}MnO_3$ single crystal that was investigated in Ref. [83] in the fields from 5 to 15 kOe, the shift of the maximum occurs with a rate of about 0.4 K kOe^{-1}, which indeed is half the rate of the displacement of the Curie temperature. The maximum value of $|\Delta S(T)|$ grows approximately proportionally to the magnetic field value. Substituting $M_\mathrm{f} = 343$ G, $H = 10$ kOe, and $\sigma_{\tau_\mathrm{C}} = 7$ K, we obtain $|\Delta S|_\mathrm{max} = 3.2$ J kg^{-1} K^{-1}. The experimental value of $|\Delta S|_\mathrm{max} = 2.45$ J kg^{-1} K^{-1} [83] is somewhat less than the calculated value, which is not surprising, since we did not take into account the presence of a demagnetizing factor.

In strong magnetic fields, the situation becomes more complex, since the difference in the magnetizations of the ferromagnetic and paramagnetic phases decreases with an increase in H, and at $H = H_\mathrm{crit}$ the jump in the magnetization disappears. Unfortunately, near the critical point the magnetocaloric effect has not been studied experimentally to date. Some theoretical results for this case are given in Ref. [83].

It follows from the above formulas that, in the case of a second-order phase transition, the smearing-out of the transition region leads only to a small decrease in $|\Delta S|$, whereas in the case of a first-order transition the magnitude of $|\Delta S|_\mathrm{max}$ is proportional to $H/\sigma_{\tau_\mathrm{C}}$ and, therefore, the role of smearing is considerably more important. Consequently, in the latter case it is possible to significantly affect the magnitude of $|\Delta S|$ by changing σ_{τ_C}. Thus, it is noted in Ref. [84] that the magnitude of the effect substantially depends on the method of preparing the samples. A study of specially prepared polycrystals of La–Ca manganites showed that the transition region in a $La_{0.7}Ca_{0.3}MnO_3$ sample is considerably narrower than in single crystals of the same composition, and in the field of 20 kOe the magnitude of ΔS reaches a value of 8 J kg^{-1} K^{-1}. We obtained above a close value of 7.1 J kg^{-1} K^{-1} with the aid of the Clapeyron equation.

4.4 Heat capacity

Let us examine, first, the region of low temperatures. At $T = 3-10$ K, the temperature dependence of the heat capacity can be presented in the following form:

$$C = \gamma T + \beta T^3 + BT^{3/2}, \qquad (13)$$

where the first term describes the electron contribution; the second term, the phonon contribution, and the third term, the magnon contribution. In sufficiently strong magnetic fields, the magnon contribution becomes negligible because of the appearance of a gap in the magnon spectrum, which makes it possible to simplify the analysis of experimental curves. In Ref. [85], the measurements on $La_{1-x}Sr_xMnO_3$ single crystals were carried out in a field $H = 90$ kOe. It turned out that the coefficient γ substantially depends on the strontium concentration: it is very small for $x \leqslant 0.1$; with increasing x, this coefficient grows to ≈ 5 mJ K^{-2} mol^{-1} at $x = 0.16$, while with a further increase in the strontium concentration the magnitude of γ only weakly depends on x and is approximately 4 mJ K^{-2} mol^{-1}.

Given the coefficient β, it is possible to calculate the Debye temperature θ_D. According to Ref. [85], the magnitude of θ_D in $La_{1-x}Sr_xMnO_3$ single crystals grows from 360 to 440 K with an increase in x from 0.1 to 0.3, after which it hardly changes.

The constant of the spin stiffness D evaluated under the assumption of a gapless magnon spectrum rapidly grows from 50 to 240 meV Å^2 with an increase in x from 0.1 to 0.2, after which it is almost independent of the strontium concentration [86].

A systematic study of the heat capacity of lanthanum–barium manganites in the low-temperature region has not, apparently, been conducted. A study of polycrystals of $La_{0.67}Ba_{0.33}MnO_3$ [87] showed that in this manganite the magnitude of γ is on the order of 5 mJ K^{-2} mol^{-1}, and the Debye temperature is approximately 400 K. The constant of spin stiffness in Ref. [87] was not determined.

The $La_{1-x}Ca_xMnO_3$ single crystals were investigated in Ref. [86]. In contrast to $La_{1-x}Sr_xMnO_3$, the dependence of γ on x has a stepped character: at $x = 0.22$, this coefficient is equal to zero; at $x = 0.225$, the magnitude of γ is equal to 4 mJ K^{-2} mol^{-1}; at $x = 0.25$, γ reaches a maximum value of 5 mJ K^{-2} mol^{-1}, after which it somewhat decreases. With an increase in the calcium content, the Debye temperature grows from 340 to 410 K. The constant of the spin stiffness is ≈ 50 meV Å^2 for $x \leqslant 0.22$ and experiences a jump at $x = 0.225$; for $x \geqslant 0.25$, $D \approx 140-150$ meV Å^2.

Although at $x \approx 1/3$ (the so-called optimum doping) the crystal structures of the manganites examined are different, and the Curie temperature of the La–Ca crystal is noticeably less than that in the La–Sr and La–Ba manganites, the magnitudes of γ and, consequently, the densities of states at the Fermi level prove to be very close.

In the region of the magnetic second-order phase transition there is a peak at $T = T_\mathrm{C}$ in the temperature dependence of heat capacity (see, e.g., the curves for a $La_{0.7}Sr_{0.3}MnO_3$ single crystal in paper [88]). The application of a magnetic field leads to a broadening of the peak and to a decrease in its height; however, no noticeable displacement of the peak under the action of the field is observed. In $La_{0.7}Ca_{0.3}MnO_3$, the magnetic transition proceeds as a first-order process; therefore, the peak is displaced toward higher temperatures. It was found in Ref. [88] that in the $La_{0.7}Ca_{0.3}MnO_3$ single

crystal this shift is on the order of 40 K in a field of 70 kOe; measurements on the $La_{0.67}Ca_{0.33}MnO_3$ polycrystal gave $dT_C/dH = 0.8$ K kOe^{-1} [76]. Above, we used the last value for evaluating $B_M = dT_C/dH$, since it is in agreement with our data on the magnetization (see Ref. [53]).

4.5 Magnetic anisotropy

The magnetic anisotropy of the lanthanum manganites was studied mainly in thin-film samples, in which a large role is played by stresses existing at the interface between the film and the substrate. Thus, it was established in Ref. [89] that the anisotropy of the epitaxial films of $La_{0.7}A_{0.3}MnO_3$, where A = Ca, Sr, Ba, or a vacancy grown on substrates of $(LaAlO_3)_{0.3}(Sr_2TaAlO_6)_{0.7}$ and $SrTiO_3$, can be described with the aid of a single constant of cubic anisotropy $K_1(T)$. The majority of data relates to films on the $(LaAlO_3)_{0.3}(Sr_2TaAlO_6)_{0.7}$ substrates. The constant K_1 is positive if A = Ca or a vacancy, and is negative if A = Sr or Ba. At low temperatures, $K_1 = 13\times\ 10^4$ erg cm^{-3} for lanthanum–calcium films; for a film with vacancies, K_1 is somewhat less, and $K_1 = -10^5$ erg cm^{-3} for lanthanum–barium film. For $La_{0.7}Sr_{0.3}MnO_3$ films, K_1 is negative, $|K_1| < 4\times10^4$ erg cm^{-3}; moreover, the value of the anisotropy constant for a film on the $SrTiO_3$ substrate is approximately two times greater than for a film grown on $(LaAlO_3)_{0.3}(Sr_2TaAlO_6)_{0.7}$ substrates.

The dependence of the magnetic anisotropy of polycrystalline $La_{1-x}Ca_xMnO_3$ ($0.125 \leqslant x \leqslant 0.19$) on the concentration of a bivalent ion was investigated in Ref. [90]. It turned out that at $x = 0.125$ and 0.15 the anisotropy is uniaxial, whereas the anisotropy of samples with $x = 0.175$ and 0.19 is cubic. The anisotropy field H_A is on the order of several kilooersteds; $H_A > 0$ for $x = 0.125$ and 0.15, and $H_A < 0$ for $x = 0.175$ and 0.19. The anisotropy constant $K_1 = H_A M_s/2$, where M_s is the saturation magnetization (for the constants of uniaxial and cubic anisotropy, we use one and the same designation). Since the magnitude of M_s is on the order of 500 G, for $|K_1|$ we obtain an estimate $|K_1| \sim 10^5$–10^6 erg cm^{-3}. The same estimate is given in Ref. [91] for a $La_{0.82}Ca_{0.18}MnO_3$ single crystal.

In single crystals of $La_{0.9}Sr_{0.1}MnO_3$ and $La_{0.8}Sr_{0.2}MnO_3$ the anisotropy is close to cubic in the low-temperature region [92]. For the anisotropy field, the following values were obtained, respectively: $H_A \approx 400$ Oe and $H_A \approx 100$ Oe, so that for a crystal with 10% Sr we obtain an estimate $|K_1| \approx 10^5$ erg cm^{-3}, and for a crystal with 20% Sr, $|K_1| \approx 2.5\times10^4$ erg cm^{-3}. It can be seen that for La–Sr single crystals the anisotropy constants are close to those obtained with thin films in Ref. [89].

Thus, the lanthanum–strontium manganites not only are characterized by a larger Curie temperature than lanthanum–calcium and lanthanum–barium compounds, but also possess anisotropy constants that are the smallest among the manganites in question, and which decrease with an increase in the strontium concentration.

5. Lattice vibrations. Phonons and magnons

5.1 Propagation of ultrasonic waves

Deviations of the structure of manganites from the ideal perovskite structure are comparatively small; in addition, the single crystals of manganites almost always consist of a large number of twins. The anisotropy of these materials, therefore, frequently can be satisfactorily described in the cubic approximation. If the propagation of elastic waves is examined, this means the involvement of elastic moduli c_{11}, c_{12}, and c_{44}.

In Refs [93, 94], the velocity of propagation of the pulses of waves with respective frequencies of 10–30 and about 800 MHz was measured. The temperature dependences of these elastic moduli were determined only for single crystals of $La_{1-x}Sr_xMnO_3$ with a strontium concentration $x \leqslant 0.175$. In should be noted that in Ref. [93] data are given for the moduli c_{11}, c_{33}, c_{44}, and c_{66} of the rhombohedral lattice at $x = 0.165$ and 0.30. All the c_{ij} moduli are characterized by a strong nonmonotonic temperature dependence; the structural transitions, just as the transition from the ferromagnetic to the paramagnetic state, are revealed from the presence of various singularities in appropriate curves. The magnetic field affects mainly the moduli $(c_{11} - c_{12})/2$ and c_{44}, which describe transverse vibrations; the bulk modulus $c_B = (c_{11} + 2c_{12})/3$ changes only a little in the magnetic field.

Studies on the propagation of ultrasonic waves at high frequencies impose stringent requirements on the quality of samples. As was noted above, the manganites are characterized by a significant inhomogeneity; therefore, experiments with the high-frequency waves often prove to be impossible. In these circumstances, the studies of frequencies of the mechanical resonance seem more efficient. For example, in Ref. [95] a single-crystalline sample with a nominal composition of $La_{0.83}Sr_{0.17}MnO_3$ with a known orientation of crystallographic axes at the frequency of approximately 1 MHz was studied. Since the temperature of the transition from the rhombohedral to the orthorhombic phase proved to be higher than the Curie temperature, the strontium concentration was in reality somewhat less than $x = 0.17$. The values of elastic moduli obtained in [95] are close to those given in Refs [93, 94].

In many studies, the composite oscillator method was applied, which is based on the measurement of the resonance frequency and quality factor of the mechanical system consisting of a sample in the shape of a rod and a piezoelectric converter glued to it. This method is suitable for the investigation of not only single-crystalline but also polycrystalline samples. The frequency of longitudinal vibrations excited in the rod is usually on the order of 100 kHz. The velocity of propagation of longitudinal waves is determined by Young's modulus E: $V_l = \sqrt{E/\rho}$, where ρ is the density. The Young modulus depends on the orientation of the axis of the cylinder relative to the crystallographic axes. In the case of a cubic crystal [96], we have

$$\frac{1}{E} = \frac{c_{11} + c_{12}}{(c_{11} + 2c_{12})(c_{11} - c_{12})} + \left(\frac{1}{c_{44}} - \frac{2}{c_{11} - c_{12}}\right) P(\mathbf{n}), \tag{14}$$

where $P(\mathbf{n}) = n_x^2 n_y^2 + n_x^2 n_z^2 + n_y^2 n_z^2$, and $\mathbf{n}$ is the unit vector along the axis of the cylinder. In Ref. [93], the following values of elastic moduli have been obtained for a $La_{0.835}Sr_{0.165}MnO_3$ single crystal at $T = 4$ K: $c_{11} = 13\times10^{11}$ erg cm^{-3}; $(c_{11} - c_{12})/2 = 4.9\times10^{11}$ erg cm^{-3}; $c_{44} = 5.9\times10^{11}$ erg cm^{-3}, so that $E = [0.085 - 0.035P(\mathbf{n})]^{-1}\times10^{11}$ erg cm^{-3}. Since $P(\mathbf{n}) \leqslant 1/3$, the second term (depending on $\mathbf{n}$) in formula (14) is an order of magnitude less than the first term. It can be assumed that this is also correct in the case of other manganite single crystals.

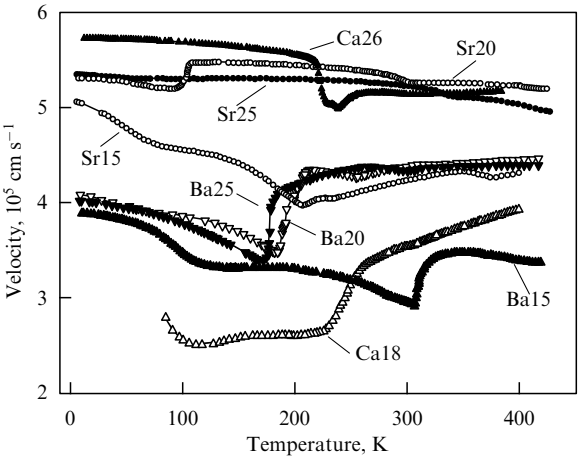

Figure 8. Temperature dependence of longitudinal sound vibrations in single crystals of lanthanum manganites, taken from Refs [53, 97–99].

Figure 8 plots the temperature dependences of the velocity of longitudinal vibrations in the single crystals of lanthanum manganites, which were given in Refs [53, 97–99]. Distinct features are quite visible in the curves, which are caused by the structural transition from the low-temperature orthorhombic to the high-temperature rhombohedral phase. The features in the curve for $La_{0.82}Ca_{0.18}MnO_3$ are connected with the transitions between two orthorhombic (O' and O^*) phases. The velocity of sound in the O' phase with strong Jahn–Teller distortions is less than that in the O^* structure, where such distortions are absent.

The transition from the ferromagnetic to the paramagnetic state has only a very weak effect on the magnitude of $V_l(T)$; it is more noticeable in the temperature dependences of the velocity of torsional vibrations [100].

The $La_{0.74}Ca_{0.26}MnO_3$ crystal represents a special case, since at $T = T_C$ there is a jump in the speed of longitudinal sound in it, which is comparable to the jump upon structural transition; moreover, V_l is greater in the ferromagnetic state than in the paramagnetic state [53].

The authors of Ref. [101] studied longitudinal vibrations in $La_{0.67}Ba_{0.33}MnO_3$ at frequencies of about 70 kHz with the use of a polycrystalline sample. The Curie temperature T_C was found to be ~ 340 K. The curve of the temperature dependence of the velocity of sound proved to be similar to those shown in Fig. 8 for the $La_{0.80}Ba_{0.20}MnO_3$ and $La_{0.75}Ba_{0.25}MnO_3$ single crystals. The structural transition, which was identified as the transition from the $R\bar{3}c$ phase to the *Imma* phase, occurred at a temperature of approximately 190 K; at the lowest temperatures, the velocity of sound was close to 4×10^5 cm s^{-1}. Apparently, the velocity of sound in $La_{1-x}Ba_xMnO_3$ for $x \geqslant 0.20$ weakly depends on the barium concentration.

Acoustic vibrations were studied in Ref. [102] in a high-quality polycrystalline sample of $La_{0.75}Ca_{0.25}MnO_3$ at frequencies of 53–55 MHz in a magnetic field of up to 40 kOe. The Curie temperature was close to 200 K. The temperature dependence of the velocity of the longitudinal waves near T_C was similar to that presented in Fig. 8 for a $La_{0.74}Ca_{0.26}MnO_3$ single crystal. In the magnetic field, the peculiarity caused by the magnetic transition is shifted toward higher temperatures at a rate that is somewhat lower than 1 K kOe^{-1}, which is in good agreement with the value of $dT_C/dH = B_M = 0.8$ K kOe^{-1} given in Section 4.2 .

In the region of phase transitions, peaks of the internal friction Q^{-1} are observed. In addition, in the $Q^{-1}(T)$ curves there are other features, at least some of which are caused by the presence of point defects [97].

The structural transitions are characterized by an extremely extensive (giant) temperature hysteresis of the velocity of sound and internal friction. The only exception is the compound $La_{0.82}Ca_{0.18}MnO_3$. In the single-crystalline $La_{0.80}Sr_{0.20}MnO_3$, the difference between the velocity of sound measured during heating and cooling is noticeable in the range from 50 to 350 K, i.e., very far from the temperature of the $Pnma - R\bar{3}c$ transition, which is ≈ 95 K [97, 98]. Consequently, the inclusions of the orthorhombic phase in the rhombohedral matrix can exist in a very wide temperature interval, which is connected, apparently, with the proximity of the thermodynamic potentials for these phases.

Using the data presented in Fig. 8, it is possible to estimate the Debye temperature. As is known [103], $k_B\theta_D = \hbar\bar{u}(6\pi^2 Nn/v)$, where N is the number of unit cells, n is the number of atoms in the unit cell, v is the volume, $3/\bar{u} = (1/V_l + 2/V_t)$, and $V_{l(t)}$ is the velocity of longitudinal (transverse) acoustic waves. For simplicity, we will assume that the unit cell is cubic with $a = 3.9$ Å, $n = 5$, the velocity of longitudinal waves will be considered equal to 5×10^5 cm s^{-1}, and V_t equal to the velocity of torsional vibrations 3.4×10^5 cm s^{-1} in a $La_{0.80}Sr_{0.20}MnO_3$ single crystal (see Ref. [100]). Then, $\bar{u} = 3.8 \times 10^5$ cm s^{-1} and the Debye temperature $\theta_D \approx 500$ K, which is in good agreement with the data on the heat capacity.

5.2 Optical phonons

In Refs [104–106], phonons in the undoped manganite $LaMnO_3$ with the orthorhombic unit cell were investigated in detail. This cell contains 20 atoms; therefore, the number of phonon branches is equal to 60, three of which are acoustic. At the point Γ of the Brillouin zone, the phonons are classified according to the irreducible representations of the group D_{2h} as follows [104, 105]:

$$\Gamma_A = B_{1u} + B_{2u} + B_{3u}\,,$$

$$\Gamma_O = 7A_g + 5B_{1g} + 7B_{2g} + 5B_{3g} + 9B_{1u} + 7B_{2u} + 9B_{3u} + 8A_u\,, \qquad (15)$$

where the Γ_A and Γ_O denote acoustic and optical modes. The mode A_u is optically inactive, but it can be investigated by the inelastic neutron scattering method.

Based on an analysis of the spectrum of the optical density of the polycrystalline $LaMnO_3$, the authors of Ref. [106] identified 14 types of vibrations. It turned out that the phonon frequencies lie in the range from 10^2 to 6.2×10^2 cm^{-1} (10^{-2} to 8×10^{-2} eV); their temperature dependence is weak.

Such a detailed description rarely proves to be possible in view of the presence of a noticeable decay of vibrations. Thus, only two bands were revealed in the optical spectra of some lanthanum manganites [107], which can be described with the aid of only two phonon frequencies: $\omega_l = 647$ cm^{-1} ($\approx 8.0\times10^{-2}$ eV) and $\omega_t = 531$ cm^{-1} ($\approx 6.6 \times 10^{-2}$ eV). The substitution of calcium, strontium, or barium for part of lanthanum only weakly influences the frequencies of phonons, since the high-frequency phonons in the lanthanum manganites are connected mainly with the vibrations of the oxygen octahedron.

Data on the dependence of phonon frequencies on the wave vector are scarce. Thus, in paper [108] dispersion curves are given (in the cubic approximation) for $La_{0.83}Ca_{0.17}MnO_3$, $La_{0.80}Ca_{0.20}MnO_3$, and $La_{0.875}Sr_{0.125}MnO_3$; in [109], experimental data are given for the rhombohedral $La_{0.80}Sr_{0.20}MnO_3$ and $La_{0.70}Sr_{0.30}MnO_3$ manganites in comparison with the results of model calculations.

5.3 Magnons

Spin waves in the manganites have been investigated by many authors. To date, the spectrum of magnons in $La_{1-x}Sr_xMnO_3$ and $La_{1-x}Ca_xMnO_3$ is well studied [110–114], whereas the data for $La_{1-x}Ba_xMnO_3$ are extremely scarce [115, 116]. The processing of experimental data is usually carried out in the cubic approximation.

Near the center of the Brillouin zone, the spectrum of spin waves is quadratic in terms of the wave vector: $\omega(q) = \Delta + Dq^2$. Since the anisotropy field is $\sim 10^3$ Oe by an order of magnitude, it can be expected that Δ has a value of 0.01–0.1 meV, i.e., it is very small. Usually, this indeed is the case, but there are exceptions. For example, according to Ref. [51], for crystals of $La_{1-x}Ca_xMnO_3$ with $0.1 \leqslant x \leqslant 0.2$ at $T = 15$ K the energy gap in the spectrum is approximately 0.2 meV, and in the case of $La_{0.83}Sr_{0.17}MnO_3$ the magnitude of the gap is $\Delta = 0.18$ meV [108].

The temperature dependence of the spin stiffness coefficient D in a wide temperature range is described by the expression $D(T) = D(0)(1 - \alpha T^{5/2})$, where $\alpha = \text{const}$ [111].

The constant of spin stiffness characterizes the spectrum of magnons only near the center of the Brillouin zone. Near the boundary of the Brillouin zone, a softening of the spectrum of spin waves occurs. Detailed data for $La_{0.75}Ca_{0.25}MnO_3$ and $La_{0.70}Ca_{0.30}MnO_3$ were published in paper [113]. The crystal lattice was assumed to be cubic. It turned out that the dependence of the magnon energy on the wave vector can be successfully described within the framework of the Heisenberg model, but it is necessary to take into account not only the exchange interaction between the nearest neighbors (i.e., along the Mn–O–Mn bond), which is described by the exchange integral J_1, but also the interaction J_4 between manganese ions in the fourth coordination shell (i.e., along Mn–O–Mn–O–Mn). The ratio J_4/J_1 is approximately equal to 0.065 in the case of $La_{0.75}Ca_{0.25}MnO_3$ and $J_4/J_1 \approx 0.20$ for $La_{0.70}Ca_{0.30}MnO_3$, so that the role of the interaction with ions in the fourth coordination shell grows with an increase in the content of calcium.

6. Magnetic resonance

Studies of the ferromagnetic (for $T < T_C$) and paramagnetic (for $T > T_C$) resonances in single crystals of $La_{1-x}D_xMnO_3$ have given similar results [52, 91, 92, 117–124]. In all cases, an anisotropy was revealed, which frequently can be considered uniaxial. The value of the g-factor is close to two, and a noticeable temperature dependence is observed at that (see, e.g., Ref. [122]). In the ferromagnetic state, lines caused by the excitation of magnetostatic waves were revealed besides the basic resonance line; the signal of the antiresonance can also be present [92]. An analysis of the data on electron paramagnetic resonance (EPR) showed that, at a temperature somewhat higher than T_C in the paramagnetic matrix, inclusions of a ferromagnetic phase exist [92, 120, 121], which is considered by some authors as evidence of the existence of the Griffith phase.

The smallest width ΔH of the basic resonance line was observed in $La_{1-x}Sr_xMnO_3$ single crystals. An increase in the content of strontium leads to a decrease in ΔH. For example, at the temperature of the transition from the ferromagnetic to the paramagnetic state, the width of the resonance line induced by the single crystals investigated in Ref. [117] is equal to 300 Oe at $x = 0.1$, whereas at $x = 0.3$, $\Delta H = 50$ Oe (at a frequency of approximately 9 GHz). Other authors give a somewhat larger value of ΔH, which is connected, most likely, with the different quality of the investigated samples.

In $La_{1-x}Ba_xMnO_3$ and $La_{1-x}Ca_xMnO_3$, the resonance line is noticeably wider than in $La_{1-x}Sr_xMnO_3$.

The temperature dependence of the width of the resonance line is similar in all the manganites under consideration. The minimum ΔH is reached near T_C. In the ferromagnetic region, a decrease in the temperature leads to an increase in ΔH, which indicates the existence of a magnetic inhomogeneity [118]. In the paramagnetic state, the removal from the point of the magnetic transition also leads to an increase in ΔH, which occurs according to a linear law: $\Delta H(T) = \Delta H(T_C) + b(T - T_C)$. The coefficient b decreases with increasing content of the doping impurity [117]. For $La_{0.7}Ba_{0.3}MnO_3$ and $La_{0.7}Ca_{0.3}MnO_3$ single crystals, the same value of $b = 2.5$ Oe K^{-1} was obtained in Ref. [122] that was found in Ref. [117] for $La_{0.7}Sr_{0.3}MnO_3$.

The width of the resonance line in $La_{1-x}Ca_xMnO_3$ single crystals sharply decreases by approximately 180 Oe in the entire investigated range of temperatures (200–600 K) when x grows from 0.18 to 0.20, whereas the width of the EPR line diminishes insignificantly with a further increase in the content of calcium [122]. This jump, just as the above-considered jumps in the electron contribution to the heat capacity and in the value of spin stiffness, is caused by changes in the electron subsystem and related changes in the exchange interactions.

The patterns in changing the width of the magnetic resonance line in the lanthanum manganites are discussed in detail by Auslender et al. [124].

The measurements of EPR spectrum can be used for the investigation of structural transitions. In Ref. [52], the EPR signal was measured in the vicinity of structural transitions in $La_{1-x}Ca_xMnO_3$ single crystals with x varying from 0.1 to 0.18, and also in $La_{0.9}Sr_{0.1}MnO_3$ and $La_{0.85}Ba_{0.15}MnO_3$. The processing of the experimental data under the assumption of the Gaussian function fitting the distribution of the concentration of the doping element made it possible to determine the standard deviation Δ of the structural transition temperature. It turned out that with increasing x in the La–Ca crystals the width of the structural transition decreases from 32 K at $x = 0.1$ to 14 K at $x = 0.18$; in the case of $La_{0.9}Sr_{0.1}MnO_3$, the standard deviation $\Delta = 33$ K. These values are in good agreement, for example, with the results of studies [97, 99]. For a $La_{0.85}Ba_{0.15}MnO_3$ single crystal, the value of Δ does not exceed 2 K, which is considerably less than follows, for example, from the results of ultrasonic measurements [98]. The reasons for this divergence are not clear.

In many manganites, the nuclear magnetic resonance (NMR) was studied. This method is one of the most informative in the study of local properties of magnetic compounds, since from the analysis of NMR spectra it is possible to obtain information about the local charge distribution. With the aid of NMR, in particular, reliable data were obtained about the charge-inhomogeneous state of manganites. In this review, we will not describe the results

obtained in this field, since they are analyzed in detail in the recent review by Mikhalev et al. [125], where references to numerous original studies are also given.

7. Transport phenomena

7.1 Basic results of band-structure calculations

The energy-band structure of $La_{1-x}D_xMnO_3$ manganites was established theoretically about 20 years ago [126–128]. As a result of the exchange interaction, the 3d levels of Mn ions are split with respect to spin (exchange splitting of ~ 3 eV). The octahedral position of Mn leads to the splitting of the 3d levels under the action of the crystal field into a group of three t_{2g}-orbitals and a group of two e_g-orbitals, with the t_{2g} levels having a lower energy. The doubly degenerate e_g levels are split due to the Jahn–Teller effect, which cause tetragonal distortions of octahedra. Electrons occupying the t_{2g} levels form a localized spin $S = 3/2$. Both the above-mentioned wave functions of Mn and (to a considerably smaller extent) the wave p-functions of oxygen participate in the formation of electron bands. The La^{3+} levels are located considerably higher than the Fermi level. In the parent $LaMnO_3$ compound, which is an antiferromagnetic insulator, the extrema of the valence band and of the conduction band are located at different points in the Brillouin zone, so that the optical gap is indirect. This conclusion is confirmed by optical experiments [129], according to which the value of the indirect gap is equal to 0.3 eV at $T = 293$ K, and to 0.4 eV at $T = 80$ K.

If the content x of a bivalent ion is approximately 1/3, then for $T \ll T_C$ the density of states at the Fermi level for electrons with the spin 'up', $N_\uparrow(E_F)$, is on the order of 1 state per eV Mn, which ensures a metallic type conductivity. For electrons with the spin 'down' there is a gap, so that such manganites are half-metallic ferromagnets. High, although not always 100%, spin polarization is confirmed experimentally (see review [130]). The Fermi surface consists of an electron spheroid in the center of the Brillouin zone and of a large hole cuboid near the point R [127]. Such a shape of the Fermi surface was revealed experimentally in studies [131, 132].

The electron structure of weakly doped manganites with a low content of bivalent ions has been studied insufficiently. We know only one study [133] in which the density of states was calculated for the compound $La_{7/8}Sr_{1/8}MnO_3$. The calculations were performed with the use of a supercell containing 16 manganese atoms. It turned out that in the region of the energy gap there are two 'impurity' peaks of the density of states, one of which is located near the top of the valence band, and the other adjoins the bottom of the conduction band. Both peaks are formed by the d-states of Mn. The Fermi level is located in the valley between the top of the valence band and adjacent 'impurity' peak, with $N(E_F) = 0$.

This picture seems to be quite natural, since in the case of a small concentration of bivalent ions the manganite can be considered a doped semiconductor. An essential feature of manganites is the presence, besides interaction with the impurity, of strong interactions of the e_g-electrons with localized spins. Calculations by the method of coherent potential carried out in Ref. [134] take into account both these interactions. At some specific choice of the parameters, the form of the density of states near the top of the valence band in the paramagnetic region calculated at $x = 0.2$ proved to be similar to $N(E_F)$ calculated in Ref. [133] for $La_{7/8}Sr_{1/8}MnO_3$: above the top of the valence band, there is an impurity peak separated from the band by a gap. This gap can disappear upon transition to the ferromagnetic state, which indicates a transition to metallic conductivity. With other choice of the parameters, the gap can exist both below and above T_C.

The reason for such a change in the density of states can easily be understood within the framework of the s–d model with a strong s–d interaction, which is usually called the double exchange model (DE model; see, for example, Refs [16, 19] and [135]). In the DE model, the hopping integral between the sites i and j depends on the angle θ_{ij} between the spins $\mathbf{S}_i$ and $\mathbf{S}_j$: $t_{ij}(\theta_{ij}) = t_{ij}\cos(\theta_{ij}/2)$. It is obvious that in this case

$$\cos\left(\frac{\theta_{ij}}{2}\right) = \frac{1}{\sqrt{2}}\sqrt{1 + \frac{\mathbf{S}_i\mathbf{S}_j}{S^2}}.$$

Let us suppose that all the spins have one and the same projection onto the z-axis, which is parallel to the magnetization $\mathbf{M}$. Then, in the spherical coordinate system, we have $\mathbf{S}_i = S(\sin\theta\cos\varphi_i, \sin\theta\sin\varphi_i, \cos\theta)$ and, similarly, for $\mathbf{S}_j$. We will assume that φ_i and φ_j are independent random variables. Calculating $\mathbf{S}_i\mathbf{S}_j$ and averaging the result with respect to φ_i and φ_j yields $\mathbf{S}_i\mathbf{S}_j/S^2 = m^2$, where $m = \cos\theta$ is the relative magnetization $m = M/M_s$, and M_s is the saturation magnetization. The bandwidth is determined by the hopping integral and, therefore, by m^2. In the region of the magnetic transition, the magnetization is small, so that $\sqrt{1+m^2} \approx 1 + m^2/2$; in other words, the bandwidth in the paramagnetic state (at $m = 0$) is approximately two thirds that in the ferromagnetic state. Consequently, if for $T > T_C$ there is a gap in the spectrum, then, upon passing to the ferromagnetic state, this gap decreases or disappears completely .

The broadening of the band upon transition to the ferromagnetic state also occurs in the broadband s–d model [135], but in this case the shift in the edge of the band is proportional to m rather than to m^2.

7.2 Resistance and magnetoresistance

The resistivity and magnetoresistance of $La_{1-x}D_xMnO_3$ single crystals have been investigated by many authors. Typical curves are demonstrated in Figs 9 and 10. In the ferromagnetic temperature range, a metal–semiconductor concentration transition occurs upon a change in x: for $x < x_c$, the temperature dependence of the resistivity $\rho(T)$ has a semiconductor nature, i.e., the resistivity grows strongly as the temperature decreases, and for $x > x_c$, the derivative $d\rho(T)/dT$ is positive (> 0), which is typical of metals. The critical concentration for $La_{1-x}Sr_xMnO_3$ is $x_c = 0.17$ [30]; for $La_{1-x}Ba_xMnO_3$, an estimate gives $0.20 < x_c < 0.25$ [45, 136–138]; and in the case of $La_{1-x}Ca_xMnO_3$, the concentration transition occurs at $x_c \approx 0.22$ [86]. If x is noticeably less than x_c, then, in the ferromagnetic region when moving away from the point of the magnetic transition, a hopping conductivity with a variable length of hopping is observed. For $x > x_c$ in this temperature range up to T on the order of 200 K, the temperature dependence of resistivity is well described as $\rho(T) = \rho(0) + AT^2$ [30, 86], which is typical of 'poor' metals. An increase in the concentration of bivalent ions leads to a decrease in A; for example, in single crystals of $La_{1-x}Sr_xMnO_3$, this coefficient decreases from $\approx 4\times 10^{-8}\ \Omega\,\mathrm{cm\ K^{-2}}$ at $x = 0.20$ to $\approx 1\times 10^{-8}\ \Omega\mathrm{cm\ K^{-2}}$ at $x = 0.40$ [30]. The residual resistivity $\rho(0)$ with increasing x also decreases. The values of $\rho(0)$ and A in the crystals of

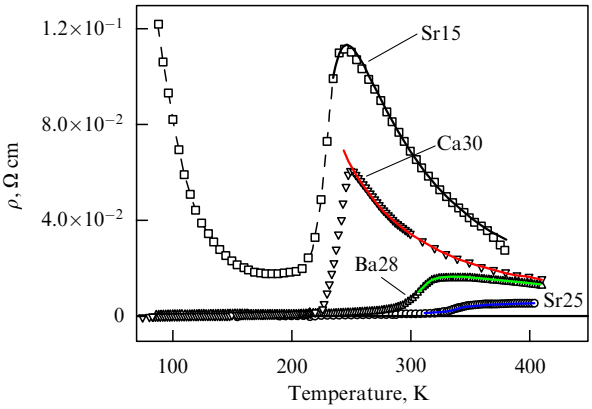

Figure 9. Temperature dependence of the resistivity of the lanthanum manganites single crystals [138, 140, 144].

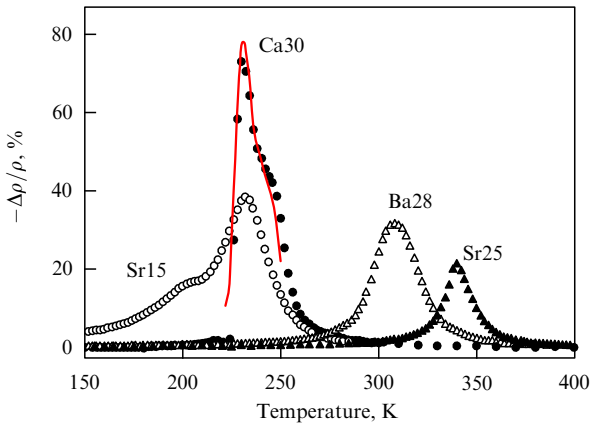

Figure 10. Magnetoresistance of the lanthanum manganite single crystals in a magnetic field $H = 10$ kOe [138, 140, 144]. Solid line corresponds to the calculated result for the magnetoresistance of the $La_{0.70}Ca_{0.30}MnO_3$ single crystal, obtained by formula (19).

$La_{1-x}Ba_xMnO_3$ and $La_{1-x}Ca_xMnO_3$ are noticeably greater than in $La_{1-x}Sr_xMnO_3$ [86, 138, 139, 45].

In the paramagnetic state, the temperature dependence of resistivity in the majority of cases has a semiconductor nature. It is natural to expect that, in the absence of a magnetic field, $\rho(T) = \rho_0 \exp(E_0/k_B T)$. This dependence is indeed observed if a first-order phase transition occurs at the Curie point (see Fig. 9). In a $La_{0.7}Ca_{0.3}MnO_3$ single crystal [140], the energy of activation $E_0 = 78$ meV, and $\rho_0 = 1.7 \times 10^{-3}$ Ω cm.

In manganites with a second-order magnetic transition, a simple exponential dependence of resistivity is observed only at a significant distance from T_C, which appears to be connected with an increase in fluctuations of the order parameter with an approach to the transition point. It is known [141] that an increase in fluctuations in ferromagnets with a weak s–d exchange leads to the appearance of singularities in the derivative $d\rho/dT$ at $T = T_C$. It can be expected that the same occurs in the manganites, and in them the derivative dE_0/dT has singularities at the transition point. It is suitable to analyze the local activation energy $\varepsilon_a = d \ln \rho / d(T^{-1})$, since $\varepsilon_a = E_0 - T(dE_0/dT)$. An analysis of data on the temperature dependence of the resistivity of different lanthanum manganites in Ref. [138] showed that

$$\varepsilon_a(T) = \varepsilon_a^{\infty} - \frac{C}{T - T_a}, \qquad (16)$$

where $C = \text{const}$, and T_a is close to the Curie temperature (more precisely, to its average value). For example, the following values were obtained for a single crystal of $La_{0.72}Ba_{0.28}MnO_3$ ($T_C = 311$ K): $\varepsilon_a^{\infty} = 0.072$ eV, $T_a = 304$ K, and $C = 2.33$ eV K.

The determination of $E_0(T)$ from the data for ε_a is, generally speaking, impossible, since the pre-exponential factor ρ_0 is unknown. It is possible, however, to take advantage of the fact that, upon moving away from the point of the phase transition, the local activation energy tends to ε_a^{∞}. Considering the expression for ε_a through E_0 as the differential equation for E_0 with the boundary condition $E_0(T \to \infty) = \varepsilon_a^{\infty}$, it can easily be found that

$$E_0 = \varepsilon_a^{\infty} + \frac{C}{T_a}\left[1 + \frac{T}{T_a} \ln\left(1 - \frac{T_a}{T}\right)\right]. \qquad (17)$$

Here, $T > T_a$. The calculation of E_0 by this formula showed [138] that E_0 and ε_a differ from each other, even at a noticeable distance from the Curie temperature [$\varepsilon_a(T = 400\,\text{K}) \approx 0.048$ eV, whereas $E_0(T = 400\,\text{K}) \approx 0.066$ eV].

The results of evaluations of the resistivity for $La_{0.85}Sr_{0.15}MnO_3$, $La_{0.7}Ca_{0.3}MnO_3$, $La_{0.72}Ba_{0.28}MnO_3$, and $La_{0.75}Sr_{0.25}MnO_3$ via the above-given formulas are shown in Fig. 9 by solid lines. The theoretical curves agree very well with the data from experiments.

Notice that the use of expression (17) makes it possible to adequately describe the temperature dependence of resistivity for $La_{0.75}Sr_{0.25}MnO_3$ as well, although in the paramagnetic region $d\rho/dT > 0$. The value $\varepsilon_a^{\infty} = 0.022$ eV proves to be, however, less than $k_B T$. To speak about the purely exponential dependence of resistivity on temperature is impossible, but the metallic conductivity also hardly occurs, the more so as the conductivity for $T > T_C$ is noticeably less than the minimum metallic conductivity $\sigma_{\min}$, which in manganites is on the order of 1 $m\Omega^{-1}$ cm^{-1} [14, 15]. The behavior of the crystals of La–Sr manganites with $x \geqslant 0.25$ resembles the behavior of gapless or narrow-gap semiconductors rather than of metals.

Near the Curie temperature, the resistivity of all manganites sharply decreases as the temperature decreases. Figure 11 illustrates the dependence of $\ln \rho(T, H = 10\,\text{kOe})$ on the square of the relative magnetization $m^2(T, H = 10\,\text{kOe})$ for crystals experiencing a magnetic transition of the second

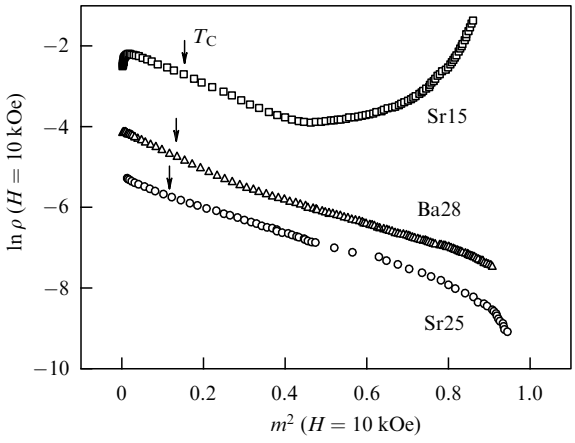

Figure 11. Dependence of the resistivity ρ measured in a magnetic field $H = 10$ kOe on the relative magnetization squared m^2 measured in the same field [138, 144].

order. Beginning with magnetization close to zero and up to $m^2 \approx 0.4$, the logarithm of ρ depends linearly on m^2. The resistivity of $La_{0.85}Sr_{0.15}MnO_3$ in the region indicated changes by a factor of five, and it changes by more than an order of magnitude in the case of the other two crystals. Hence, the decrease in the resistivity in the region of the transition is a consequence of a decrease in the activation energy E_a; in other words, in this region one obtains $E_a = E_0 - E_1 m^2$, so that

$$\rho = \rho_0 \exp\left(\frac{E_0 - E_1 m^2}{k_B T}\right), \tag{18}$$

where E_0 depends on temperature as was described above. The data on the $E_1(T)$ dependence are scarce; apparently, this dependence is weak [138]. Simple estimations show that E_1 is on the order of 0.1 eV.

In the magnetic field, the activation energy decreases, so that the magnetoresistance

$$\frac{\Delta\rho}{\rho} = \frac{\rho(H) - \rho(0)}{\rho(0)}$$

proves to be negative. From formula (18), it follows that

$$\frac{\Delta\rho}{\rho} = \exp\left[-\frac{E_1\left(m^2(H) - m^2(0)\right)}{k_B T}\right] - 1\,.$$

In a weak magnetic field, a change in the magnetization is small; therefore, one has

$$\frac{\Delta\rho}{\rho} = -\frac{E_1}{k_B T}\left[m^2(H) - m^2(0)\right].$$

The quadratic dependence of the magnetoresistance on the magnetization has been observed in many materials [141]; for lanthanum–strontium manganites, it was established in Ref. [30]. Detailed data for the $La_{1-x}Ba_xMnO_3$ single crystals are reported in paper [45].

In manganites with the first-order magnetic transition, formula (18) is valid only in the paramagnetic region, where the magnetoresistance is small. Large values of $\Delta\rho/\rho$ are observed near the Curie temperature, or, to be more precise, near its average value. We will assume that the values of the local Curie temperature $\tau_C(\mathbf{r})$ lie in the region whose width δ_c is much less than $T_C = \langle\tau_C\rangle$. In the region of the magnetic transition, the resistivity depends on the difference $T - \tau_C(\mathbf{r})$; the noncritical contribution to ρ is a smooth function of temperature. In the magnetic field, the resistivity depends on H due to changes in the probability of scattering, concentration of charge carriers, etc., and also because of the shift in the transition temperature in the magnetic field.

The resistivity is, therefore, a functional of $T - \tau_C(\mathbf{r})$: $\rho(T) = F_{T,H}\{T - \tau_C(\mathbf{r})\}$, where the subscripts indicate the presence of a noncritical dependence on T and H. The shift in the transition temperature can be considered to be independent of $\mathbf{r}$. We will also assume that the change in the noncritical contribution to the resistivity in the temperature range under consideration can be ignored. Then, the following relationship holds true:

$$\begin{aligned}\rho(T,H) &= F_{T=T_C,H=0}\left\{T - \tau_C(\mathbf{r}, H=0) - \Delta T_C(H)\right\}\\ &= \rho\left(T - \Delta T_C(H), H=0\right),\end{aligned}$$

where $\Delta T_C(H) = B_M H$, and we arrive at a simple formula for the magnetoresistance:

$$\frac{\Delta\rho(T,H)}{\rho} = \frac{\rho\left(T - \Delta T_C(H)\right) - \rho(T)}{\rho(T)}\,, \tag{19}$$

where $\rho(T) = \rho(T, H=0)$. It has been shown in Ref. [139] that this formula well describes the dependence of the magnetoresistance of a $La_{0.7}Ca_{0.3}MnO_3$ single crystal on temperature in a constant magnetic field. Consequently, in the region of a first-order magnetic transition, the shape of the $\Delta\rho(T, H = \text{const})/\rho$ curve is determined by the temperature dependence in a zero field and by the shift in the Curie temperature in the magnetic field.

The assumptions made can easily be understood if we take into account that near T_C there is a mixture of the metallic ferromagnetic and semiconductor paramagnetic phases in the sample. The application of a magnetic field causes an increase in the volume of the metallic phase as a result of the shift in the transition temperature and, therefore, a decrease in the resistivity. These assumptions mean disregarding the temperature and magnetofield dependences of the resistivity of the phases indicated. Previously, similar approximations were made by us in describing the magnetocaloric effect.

The above considerations about the origin of the magnetoresistance of manganites are phenomenological and say nothing about the nature of the parameters used to describe the dependence of $\Delta\rho/\rho$ on the temperature and magnetic field value. It can easily be shown, however, that the dependence of the activation energy on the magnetization is similar to the dependence of the width of the electron energy band. It can, therefore, be assumed that the crux of the matter lies in the reconstruction of the electron energy-band structure upon changing the state of the magnetic subsystem in the crystal.

7.3 Hall effect

In ferromagnetic materials, the Hall effect is determined not only by the induction B of the magnetic field in the sample, but also by the magnetization [142]:

$$\rho_H = R_0 B + R_s M\,, \tag{20}$$

where ρ_H is the Hall resistivity, and R_0 and R_s are the normal (ordinary) and anomalous (spontaneous, extraordinary) Hall coefficients. Measurements of the Hall effect are usually conducted using samples in the form of thin plates; therefore, the induction B may be considered to be equal to the external field H.

For $T \ll T_C$, the magnetization is almost independent of the field, so that the second term on the right-hand side of formula (20) can be assumed to be equal to $R_s M_s$, where M_s is the saturation magnetization. In this case, the Hall coefficients can easily be determined by plotting the curve of the dependence of ρ_H on H, which is usually indeed done. With an increase in the temperature, the dependence of the magnetization on the field becomes essential, and the Hall coefficient is conveniently determined from the curves of the dependence of ρ_H/H on M/H. In the paramagnetic region, $M = \chi H$, so that $\rho_H = (R_0 + \chi R_s)\,H = R_{\text{eff}} H$. In this case, it is impossible to determine R_0 and R_s from the dependence of ρ_H on H. However, if R_0 and R_s weakly (in comparison with χ) depend on temperature, then it is possible to find them by constructing the dependence of R_{eff} on χ.

Experimental Hall-effect data obtained on single-crystalline samples are comparatively scarce. The first measurements (see paper [143]) were carried out on single crystals of $La_{1-x}Sr_xMnO_3$ ($0.18 \leqslant x \leqslant 0.50$). Later on, papers [144–146] appeared, in which single crystals of La–Sr, La–Ba, and La–Ca compounds were investigated; similar data were published in Refs [147, 148] for $Nd_{1-x}Sr_xMnO_3$ crystals. The main results obtained in these studies are the following.

The anomalous Hall coefficient in all the manganites is negative. The magnitude of R_s increases with an approach to the point of the phase transition, and near T_C it exceeds R_0 by one–two orders of magnitude, which indicates the presence of strong spin–orbital interaction. In metals, the connection between the anomalous Hall coefficient and resistivity can be presented in the form [149, 150]

$$R_s = a_1\rho + a_2\rho^2\,, \tag{21}$$

where the constants a_1 and a_2 describe the contribution of the asymmetric (skew) scattering and lateral (side jump) displacement. If the conductivity in the ferromagnetic state is metallic, and $\rho(T) = \rho(0) + AT^2$, then in manganites the dependence of R_s on ρ is usually (but not always: see Ref. [143]) close to linear. In the paramagnetic region, the anomalous Hall coefficient remains negative in the vicinity of T_C and is large in magnitude [138, 144]. But if a semiconductor type conductivity is realized for $T < T_C$, as, for example, in $La_{0.85}Sr_{0.15}MnO_3$ [144], then the behavior of R_s with varying ρ can be described by the formula obtained in Ref. [145]:

$$R_s = \rho_{xy}^{(0)}\,\frac{(1-m^2)^2}{(1+m^2)^2}\,, \tag{22}$$

where $\rho_{xy}^{(0)} = \text{const}$; no data are available for the paramagnetic region.

The temperature behavior of the normal Hall coefficient depends on the level of doping and the type of magnetic phase transition. In the crystals of $La_{1-x}Sr_xMnO_3$ with $x > x_c$, the coefficient R_0 is positive in the ferromagnetic range of temperatures [143, 144]. The dependence of R_0 on the content of Sr in the interval of $0.18 < x < 0.5$ is weak. If we assume that $R_0 = 1/en_{\text{eff}}$, then for the charge-carrier concentration one obtains a value $n_{\text{eff}} \sim 10^{22}$ cm^{-3}, which corresponds to one–two holes per strontium ion; this is considerably greater than would be possible to expect based on the doping level. Obviously, such a small value of R_0 indicates the presence not only of a hole, but also of an electron contribution, which is in agreement with the results of calculations of the band structure given in Section 7.1. In a $La_{0.72}Ba_{0.28}MnO_3$ single crystal, the normal Hall coefficient is negative for $T < 145$ K, which indicates a larger role of electrons in this manganite [138]. With the growth in temperature, R_0 increases; near T_C, this increase becomes sharper. If a semiconductor type of conductivity is realized in the ferromagnetic state, i.e., if $x < x_c$, then, at low temperatures, R_0 is less than zero [136–138, 144]; however, when approaching the Curie temperature, it can become positive.

An increase in R_0 as $T \to T_C$ is observed only if the magnetic transition is a second-order one. However, if magnetic transition is a first-order transition, as in the case of $La_{0.70}Ca_{0.30}MnO_3$, then the growth of R_0 in the vicinity of T_C is absent [139, 144].

Important information about the mechanisms of conductivity can be obtained from data on the temperature dependence of the Hall mobility $\mu_H = R_0/\rho$. Figure 12 plots the temperature dependence of μ_H for $La_{0.80}Sr_{0.20}MnO_3$ ($T_C = 308$ K) and $La_{0.70}Ca_{0.30}MnO_3$ ($T_C(0) = 227$ K) single crystals. In $La_{0.80}Sr_{0.20}MnO_3$, up to the temperature of ≈ 200 K, i.e., where $\rho(T) = \rho(0) + AT^2$, the temperature dependence of the mobility is typical of a 'poor' metal, in which the majority carriers are holes, and the resistivity is caused by the decrease in their mobility. However, above 200–250 K, the mobility is almost independent of T and small in magnitude, $\mu_H \approx 0.3$ cm^2 V^{-1} s^{-1}, so that the main contribution to the conductivity comes from the charge carriers with an energy close to the mobility edge [151], and an increase in resistivity is caused by a decrease in the concentration of charge carriers in the delocalized states. Hence, it follows that the metal–semiconductor transition takes place in the temperature interval of 200–250 K, rather than at a temperature that corresponds to the maximum of resistivity, which in our case is equal to about 340 K.

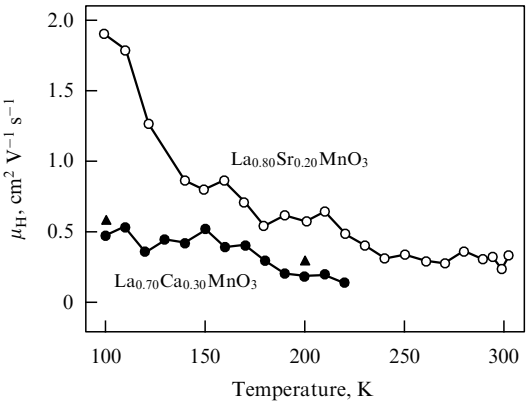

Figure 12. Hall mobility in the $La_{0.80}Sr_{0.20}MnO_3$ ($T_C = 308$ K; open symbols, the data from Ref. [144]) and $La_{0.70}Ca_{0.30}MnO_3$ ($T_C(0) = 227$ K; filled circles, data from Ref. [140]; filled triangles, the data from Ref. [145]) single crystals.

In a $La_{0.70}Ca_{0.30}MnO_3$ single crystal, the mobility decreases monotonically, which indicates the metallic nature of conductivity up to the temperature $T = 220$ K, at which a sharp increase in the resistivity begins.

If in the ferromagnetic state the conductivity is that of a semiconductor, then the mobility $\mu_H < 0$ and it is small (on the order of 0.1 cm^2 V^{-1} s^{-1} or less), which, as is known [151], indicates a hopping conductivity.

Data on the Hall effect in the paramagnetic region far from the Curie temperature are extremely scarce. For the $La_{0.70}Ca_{0.30}MnO_3$ single crystal at $T = 400$ K, i.e., sufficiently far from the Curie point, the coefficient R_{eff} is on the order of -10^{-9} Ω m T^{-1} [139, 140]. The resistivity of the crystal at 400 K is approximately 10^{-2} Ω cm. If we assume that R_{eff} at this temperature is completely determined by R_0 and that the anomalous Hall effect can be disregarded, then the following estimate is obtained: $\mu_H \sim -0.1$ cm^2 V^{-1} s^{-1}. The magnitude and the sign of μ_H indicate that for $T \gg T_C$ a hopping conductivity is realized between the nearest neighbors.

7.4 Thermopower

The thermal emf S and its dependence on the temperature and magnetic field have been studied by many authors. Let us examine first the $S(T, H)$ dependence in manganites with a second-order magnetic transition. There are detailed data for

$La_{1-x}Sr_xMnO_3$ single crystals [144, 152, 153]. In the case of $La_{0.85}Sr_{0.15}MnO_3$ ($x < x_c$), the thermal emf is positive at almost all temperatures, except for $T < 50$ K. In the $S(T)$ curve, there are two maxima, the first of which is located at $T \approx 100$ K, while the second lies somewhat higher than the Curie temperature T_C. The maximum value S_{max}, according to Ref. [144], is equal to 56 μV K^{-1}, whereas, according to Ref. [153], $S_{max} = 35$ μV K^{-1}. The difference between two values is most likely due to a small difference in the strontium content. In the samples with $x > x_c = 0.17$, the value of the thermal emf is significantly less, the maximum at $T = T_C$ is pronounced weakly, and for $x > 0.20$ it is completely absent. Although the ferromagnetic manganites with the bivalent ions content $x < 0.5$ are usually considered materials with hole conductivity, in crystals with $x = 0.20$ and 0.25 the sign of S is positive only in the ferromagnetic temperature range, whereas for $T > T_C$ the thermal emf is negative. In crystals with the strontium content $x = 0.4$, the thermal emf is negative at all temperatures [152]. Notice that the normal Hall coefficient remains in this case positive [143].

The application of a magnetic field leads to a decrease in $|S|$, which is most significant near the Curie temperature, where the difference $\Delta S = S(H) - S(0)$ is proportional to the square of the relative magnetization: $\Delta S \sim m^2$.

Similar dependences are characteristic of the $La_{1-x}Ba_xMnO_3$ single crystals [136–138, 154].

If a first-order magnetic transition takes place, as in a $La_{0.70}Ca_{0.30}MnO_3$ single crystal [140], then the dependence of the thermal emf on the temperature and magnetic field is different. In the $S(T)$ curve near the Curie temperature, there is a sharp maximum, which is absent in the La–Sr and La–Ba crystals with the same level of doping. This maximum is not suppressed by a magnetic field, but is only shifted toward larger temperatures, which is caused by the shift in the temperature of the transition in a magnetic field. In the region of transition, the dependence of S on T and H is determined by the co-existence of the low-temperature (lt) ferromagnetic and high-temperature (ht) paramagnetic phases; in the region of transition, this dependence is well described by a simple formula derived in Ref. [155]:

$$S(T,H) = \frac{1}{\rho_{ht}(T) - \rho_{lt}(T)} \left[\rho_{ht}(T)\, S_{lt}(T) - \rho_{lt}(T)\, S_{ht}(T) + \rho(T,H)\big(S_{ht}(T) - S_{lt}(T)\big)\right], \quad (23)$$

where $\rho(T,H)$ is the resistivity of the sample in a magnetic field, and $\rho(T) = \rho(T, H = 0)$.

In all cases, the dependence of S on T in the paramagnetic region is well described by the relationship

$$S = \frac{k_B}{e}\left(\frac{E_a^S}{k_B T} + A^S\right), \quad (24)$$

where $k_B/e \approx 87$ μV K^{-1}, E_a^S is the energy of activation for the thermal emf, and A^S is a constant on the order of unity. For example, in the case of $La_{0.70}Ca_{0.30}MnO_3$, this activation energy $E_a^S = 12$ meV, $A^S = -0.47$ [140]; similar values were obtained for other manganites. It should be emphasized that the value of the activation energy is noticeably lower than $k_B T$. This cannot be understood if we assume that the thermal emf and resistivity are caused by electrons in the conduction band or by holes in the valence band. But if we accept, in accordance with data on the Hall effect, that in the paramagnetic state a hopping conductivity takes place, then the features indicated obtain a natural explanation, since in this case E_a^S is caused by the asymmetry (though small) of the density of states near the Fermi level [156].

The singularities caused by magnetic and structural transitions are also observed in the temperature dependences of the coefficient of thermal conductivity measured in the polycrystalline and single-crystalline samples of $La_{1-x}Sr_xMnO_3$ [153, 157], and in the $La_{1-x}Ca_xMnO_3$ polycrystals [158].

8. Optical properties

Important information about the electron band structure can be obtained from the study of optical properties; however, the number of articles devoted to the optics of manganites is rather small.

The most detailed data are available for single crystals of $La_{1-x}Sr_xMnO_3$ [159–163]. For the photon energy $\hbar\omega > 6$ eV, wide maxima were revealed in the spectral dependence of the dielectric constant ε_2 at energies of approximately 25, 17, and 8 eV. The position of these peaks is practically independent of x [159]. For $\hbar\omega < 6$ eV, in curves of the dependence of the optical conductivity σ_{opt} on the frequency there are two wide peaks at energies of approximately 2 and 4.5 eV; in this region, an essential dependence of spectra on the strontium concentration and on the temperature is observed. If $\hbar\omega$ is less than ≈ 1 eV, then, in the case of undoped $LaMnO_3$, the absorption is very small, which indicates the presence of a direct gap in the electron band spectrum; however, the true absorption edge is formed, as was noted above, by indirect transitions (see Ref. [162]). The substitution of strontium for part of the lanthanum leads to a shift in the peaks toward smaller energies and to an increase in σ_{opt}. When $\hbar\omega < 0.1$ eV, the interaction with lattice vibrations prevails in the spectrum.

The interpretation of optical spectra is usually based on the analysis of optical transitions in complexes formed by the manganese ion and by surrounding oxygen ions, rather than on the basis of existing band calculations. The exception is Ref. [162], where the experimental spectrum of the optical conductivity of a $La_{0.7}Sr_{0.3}MnO_3$ single crystal is compared with the results of calculations based on the data of Ref. [128].

If $x > x_c$, then, for $T \ll T_C$, a quasi-Drude increase is observed in the optical conductivity with a decrease in the frequency, which is caused by the presence of metallic conductivity. In the paramagnetic region, the quasi-Drude peak is absent even if the temperature dependence of the resistivity has a characteristic 'metallic' form, i.e., $d\rho/dT > 0$, as in the case of $La_{0.6}Sr_{0.4}MnO_3$ [163]. A decrease in the temperature leads to a gradual increase in the optical conductivity; a distinct quasi-Drude behavior in this single crystal ($T_C = 366$ K) is observed only for $T < T^*$, where T^* is approximately equal to room temperature. For a single crystal of $La_{0.825}Sr_{0.175}MnO_3$ with the Curie temperature $T_C = 283$ K, the value of T^* is on the order of 200 K [160]. It can be seen that these data completely agree with the results of our analysis of transport phenomena.

Similar results were obtained for the $La_{1-x}Ba_xMnO_3$ single crystals [164].

In the $La_{0.7}Ca_{0.3}MnO_3$ manganite, in which the magnetic transition is of the first order, the evolution of the optical spectra has a sharper character. In Ref. [165], results of measurements of the optical spectra of a $La_{0.7}Ca_{0.3}MnO_3$ film with a thickness of 165 nm ($T_C = 256$ K) are given. For

$T \geqslant 255$ K, the $\sigma_{opt}(\omega)$ curves have the shape characteristic of the semiconductor state, whereas already at $T = 245$ K the shape of the curve is completely similar to that observed in $La_{0.6}Sr_{0.4}MnO_3$ and $La_{0.825}Sr_{0.175}MnO_3$ samples at considerably lower temperatures.

The above results show that for $\hbar\omega < 6$ eV the optical properties of CMR manganites strongly depend on the state of the magnetic subsystem. Near the Curie temperature, this state changes upon applying even a comparatively weak magnetic field, which should lead to a substantial dependence of light absorption and reflection on H. Such effects, called giant magnetotransmission and magnetoreflection, are indeed observed and have prospects for practical applications [166, 167]. Unfortunately, the dependence of these effects on the parameters of the magnetic subsystem has thus far been studied insufficiently.

Because of the presence of different kinds of inhomogeneities in manganites, metallic and semiconductor regions can coexist in them in a certain temperature range. This coexistence frequently is considered a 'phase separation.' The question arises about the ratio of the volumes of these regions and about whether the effect of colossal magnetoresistance is connected with this 'phase separation'. In papers [168, 164], it was shown that a study of the optical absorption of CMR manganites in the region of interaction of light with the charge carriers makes it possible to give an answer to this question.

The idea consists in a comparison of the temperature dependences of the static conductivity $\sigma_{dc} = 1/\rho$ and of the absorption coefficient α. The studies were carried out on single crystals with $x < x_c$. In the paramagnetic region, the $\sigma_{dc}(T)$ and $\alpha(T)$ dependences have an identical character: upon cooling from room temperature to T_C, the absorption coefficient decreases as in semiconductors, while for $T < T_C$, the absorption grows as in conducting materials. Since in the ferromagnetic state the resistivity of the investigated crystals increases upon a decrease in T, an increase in the absorption can be explained only by the presence of regions with 'metallic' conductivity, which are separated from each other by the semiconductor matrix and therefore do not make a noticeable contribution to σ_{dc}. On the assumption that the conductivity in metallic droplets is, by the order of magnitude, equal to the minimum metallic conductivity σ_{min}, which is on the order of 1 $m\Omega^{-1}$ cm^{-1}, the authors of Ref. [168] estimated the relative volume $\Delta v/v$ of metallic regions in some weakly doped manganites. It turned out that in $La_{0.9}Sr_{0.1}MnO_3$, even at $T = 100$ K, the volume of the metallic phase is only 0.2% of the volume of the sample; in crystals with a smaller content of bivalent ions, the magnitude of $\Delta v/v$ is noticeably less. For $La_{0.85}Ba_{0.15}MnO_3$, a value of $\Delta v/v = 0.6\%$ was obtained in a similar manner at $T = 190$ K [164]. Near the Curie temperature, where colossal magnetoresistance is observed, the content of the metallic phase is still less. Hence it follows that the CMR effect is not connected with the appearance of metallic droplets.

An analysis of optical properties made it possible to clear up the problem of the existence and of the role of polaron type carriers in the manganites. In the article by Mostovshchikova [169], the optical properties (reflection coefficients $R(\omega)$ and absorption coefficients $\alpha(\omega)$) of $La_{1-x}A_xMnO_3$ single crystals with A = Sr, Ca, and Ba were considered for temperatures $T > T_C$. The basic feature of the reflection spectra for the manganites, which contained no more than 15% substitutional ions, is the weak dependence of the reflection coefficient on energy in the region of $\hbar\omega > 0.1$ eV. This form of dependence is characteristic of materials with the polaron type conductivity, in particular of ferrites [170] and titanates of barium [171]; therefore, an assumption was made that the polarons play the main role in the manganites indicated as well. The use of known theoretical formulas for the electrostatic polarons of a small radius made it possible with a good accuracy to describe the reflection spectrum and to determine the activation energy of polarons E_a^{pol}. The obtained values of E_a^{pol} were used for calculating the absorption spectra, which were then compared with the experimental spectra. The calculated $\alpha(E)$ curves for $La_{0.92}Ca_{0.08}MnO_3$ and $La_{0.85}Ba_{0.15}MnO_3$ manganites practically coincide with the experimental curves in the region of $\hbar\omega > 0.16$ eV. For $La_{0.93}Sr_{0.07}MnO_3$, the difference between the experimental and calculated values of the absorption coefficient is noticeable, and in the case of $La_{0.85}Sr_{0.15}MnO_3$ (for the La–Sr manganites, $x_c = 0.17$), the calculated and experimental $\alpha(\omega)$ curves diverge significantly. This indicates that in a $La_{0.85}Sr_{0.15}MnO_3$ single crystal, whose resistivity is small, the small-radius polarons are not the majority charge carriers.

A comparison of the values of the activation energy for electrical resistivity, E_0 and E_a^{pol}, showed that the radius of the wave function of a polaron is more than the distance to the neighbors that are nearest to Mn (oxygen ions), so that more than one Mn ion participates in the formation of a polaron. Hence it follows that the polarons in manganites are not purely electrostatic, and that exchange interaction between the Mn moments makes a certain (most likely small) contribution to E_a^{pol}. The magnetic moment of such a complex is different both from the Mn^{3+} moment and from the Mn^{4+} moment. The correlation length decreases with an increase in the temperature, which must lead to a decrease in the magnetic moment of the polaron, so that at temperatures that are much higher than T_C, the moments of Mn ions are independent of one another. Specifically, it is precisely such a behavior of the effective magnetic moment that follows from the analysis of the temperature dependence of the magnetic susceptibility in a number of manganites [172,173].

Let us emphasize that polarons of the type indicated are the majority charge carriers only in the case of weak doping. The reason appears to lie in the fact that an increase in the number of bivalent ions leads to an overlap of the wave functions of separate polarons.

9. Conclusions

The variety of crystalline phases revealed in manganites of various compositions and the low value of the heat of structural transitions indicate the proximity of the energy of these phases. This proximity is the natural consequence of the fact that the crystal lattice of manganites is, in essence, a relatively weakly distorted perovskite lattice, so that in the very rough approximation it is possible to consider it a cubic lattice. The weakness of the distortions of the perovskite structure is supported by the fact that the magnetic anisotropy in many instances is well described as cubic.

The proximity of the energy of the crystal structures generated by the distortion of a perovskite lattice leads to a high sensitivity of the crystal structure of manganites to details of the processes of synthesis and of heat treatment of the samples, and also to small deviations from the stoichiometric composition. As a consequence, very different crystal structures have been discovered in manganites: from cubic to

monoclinic. During the construction of the phase diagrams, we used the data that were considered to be most reliable.

The phase transition from the ferromagnetic to the paramagnetic state in the manganites can be not only of the second order, as in $La_{1-x}Sr_xMnO_3$ and $La_{1-x}Ba_xMnO_3$, but also of the first order, as in $La_{1-x}Ca_xMnO_3$ for $x \geqslant 0.25$ and in a number of other crystals. The structural inhomogeneity inherent in all manganites leads to a magnetic inhomogeneity and smearing out of the transition as a result of the spread in the values of the Curie temperatures. Therefore, the indication of the average value of T_C, to which almost all authors are limited, is completely insufficient for this reason: it is necessary to indicate the standard deviation σ_{τ_C} for the Curie temperature. Our estimates show that the most uniform materials are the $La_{1-x}Sr_xMnO_3$ single crystals, in which σ_{τ_C} is approximately 1 K, and the most inhomogeneous crystals are $La_{1-x}Ca_xMnO_3$, for which σ_{τ_C} is on the order of 5–7 K. In the case of a strong smearing-out of the magnetic phase transition, the use of the well-known Banerjee criterion for determining the type of transition can lead to incorrect conclusions.

The spectrum of magnons in the manganites can be successfully described within the framework of the Heisenberg model, but it is necessary to take into account the exchange interaction not only between the nearest neighbors (i.e., along the Mn–O–Mn bonds), but also between the manganese ions in the fourth coordination shell along the Mn–O–Mn–O–Mn bonds.

The main features of the thermodynamic characteristics and of transport phenomena are due to the strong interaction of charge carriers with the magnetic subsystem of the crystal; therefore, the behavior of the resistivity and thermal emf is determined by the magnitude of the magnetization and by spin correlations. In the paramagnetic region, as a rule, a hopping conductivity is realized between the nearest neighbors with a temperature-independent activation energy. If the number of Mn^{4+} ions is small, then the charge carriers are electrostatic polarons, whose activation energy contains a contribution from the interaction between manganese ions. In the far ferromagnetic region, the temperature dependence of the resistivity has a form typical of 'poor' metals and is characterized by low (on the order of 1 $cm^2\ V^{-1}\ s^{-1}$) mobility if the concentration of bivalent ions is higher than the critical value, $x > x_c$. If $x < x_c$, then the temperature dependence of the resistivity has a semiconductor form; in some cases, a variable-range hopping conductivity is realized.

The character of the change in the resistivity upon magnetic transition depends on the type of transition, i.e., whether it is of the first or of the second order. In the case of a first-order transition, the manganite in the ferromagnetic phase is a metal, while in the paramagnetic phase, a semiconductor, so that the magnetic transition is, simultaneously, a metal–semiconductor one. In the region of the transition, the metallic and semiconductor phases coexist. The magnetoresistance $\Delta\rho/\rho$ in this case is determined by the temperature dependence of the resistivity in a zero magnetic field and by the shift in the Curie temperature in the magnetic field.

In the case of a second-order magnetic transition, the situation is different. As the temperature approaches T_C from the paramagnetic phase, an increase in spin fluctuations occurs, which leads to a decrease in the resistivity as a result of the decrease in the activation energy E_a; the temperature dependence $E_a(T)$ has a critical character in this case. The transition to an ordered state leads to a further decrease in the activation energy, which is described by the relationship $E_a(T) = E_0 - E_1 m^2(T)$. Such a behavior of E_a leads to a maximum of the resistivity at a temperature somewhat higher than T_C. An analysis of the results of measurements of the resistivity and of the Hall effect taking into account optical data shows that the manganite resides in this case in a semiconductor state, and the peak of the resistivity is not an indication of the metal–semiconductor transition, which occurs in the ferromagnetic region at a substantial distance from the Curie temperature. The high value of $\Delta\rho/\rho$ in the vicinity of T_C (i.e., the effect of colossal magnetoresistance) is caused by a change in the activation energy in the magnetic field.

It was stated in many studies that the CMR effect is a consequence of the appearance of metallic droplets in the semiconductor matrix, and the magnetoresistance appears because of an increase in the volume of these droplets in the magnetic field. The data given in this survey show that this is correct only in the case of first-order magnetic transition. In the case of manganites with the second-order magnetic phase transition, the volume of metallic inclusions in the region of the transition is, according to optical data, noticeably less than 1% and, consequently, a change in the volume of these inclusions cannot be the reason for the CMR effect. An increase in the volume of droplets and the formation of a singly connected metallic region occur only in the ferromagnetic region.

The results of optical studies show that a change in the properties of manganites occurs because of a reconstruction of the electronic spectrum and the disappearance of the energy gap upon the transition to the ferromagnetic phase. Hence it follows that a consistent theory of the CMR effect must take into account the presence of at least two electron bands.

Acknowledgments

The authors are grateful to their friends and co-authors N N Loshkareva, E V Mostovshchikova, Yu P Sukhorukov, and E A Gan'shina for the numerous discussions of the properties of CMR manganites.

The work was performed within the framework of the state assignment to FANO of the Russian Federation (theme: Spin, No. 01201463330) and the Program No. 15-12-2-17 of the Ural Branch of the Russian Academy of Sciences.

References

1. Jonker G H, van Santen J H *Physica* **16** 337 (1950)
2. Zener C *Phys. Rev.* **82** 403 (1951)
3. Anderson P W, Hasegawa H *Phys. Rev.* **100** 675 (1955)
4. de Gennes P-G *Phys. Rev.* **118** 141 (1960)
5. Methfessel S, Mattis D C, in *Handbuch der Physik* Vol. 18 (Ed. H P J Wijn) (Berlin: Springer, 1968) p. 389
6. von Helmholt R et al. *Phys. Rev. Lett.* **71** 2331 (1993)
7. Jin S et al. *Science* **264** 413 (1994)
8. Kagan M Yu, Khomskii D I, Mostovoy M V *Eur. Phys. J. B* **12** 217 (1999)
9. Kugel K I et al. *JETP* **98** 572 (2004); *Zh. Eksp. Teor. Fiz.* **125** 648 (2004)
10. Kugel K I et al. *Phys. Rev. B* **78** 155113 (2008)
11. Dagotto E *New J. Physics* **7** 67 (2005)
12. Fäth M et al. *Science* **285** 1540 (1999)
13. Uehara M et al. *Nature* **399** 560 (1999)
14. Coey J M D, Viret M, von Molnár S *Adv. Phys.* **48** 167 (1999)
15. Salamon M B, Jaime M *Rev. Mod. Phys.* **73** 583 (2001)

16. Izyumov Y A, Skryabin Yu N *Phys. Usp.* **44** 109 (2001); *Usp. Fiz. Nauk* **171** 121 (2001)
17. Kagan M Yu, Kugel' K I *Phys. Usp.* **44** 553 (2001); *Usp. Fiz. Nauk* **171** 577 (2001)
18. Dagotto E *Nanoscale Phase Separation and Colossal Magnetoresistance* (Berlin: Springer-Verlag, 2003)
19. Edwards D M *Adv. Phys.* **51** 1259 (2002)
20. Dunaevskii S M *Phys. Solid State* **46** 193 (2004); *Fiz. Tverd. Tela* **46** 193 (2004)
21. Goodenough J B *Rep. Prog. Phys.* **67** 1915 (2004)
22. Gor'kov L P, Kresin V Z *Phys. Rep.* **400** 149 (2004)
23. Tokura Y *Rep. Prog. Phys.* **69** 797 (2006)
24. Aksenov V L, Balagurov A M, Pomyakushin V Yu *Phys. Usp.* **46** 856 (2003); *Usp. Fiz. Nauk* **173** 883 (2003)
25. Bebenin N G *Phys. Met. Metallogr.* **111** 236 (2011); *Fiz. Met. Metalloved.* **111** 242 (2011)
26. Krivoruchko V N *Low Temp. Phys.* **40** 586 (2014); *Fiz. Niz. Temp.* **40** 756 (2014)
27. Hwang H Y et al. *Phys. Rev. Lett.* **77** 2041 (1996)
28. Gupta A et al. *Phys. Rev. B* **54** R15629 (1996)
29. Koohpayeh S M, Fort D, Abell J S *Prog. Cryst. Growth Charact. Mater.* **54** 121 (2008)
30. Urushibara A et al. *Phys. Rev. B* **51** 14103 (1995)
31. Balbashov A M et al. *J. Cryst. Growth* **167** 365 (1996)
32. Shulyatev D et al. *J. Cryst. Growth* **237 – 239** 810 (2002)
33. Shulyatev D et al. *J. Cryst. Growth* **291** 262 (2006)
34. Prabhakaran D et al. *J. Cryst. Growth* **237 – 239** 806 (2002)
35. Tofield B C, Scott W R *J. Solid State Chem.* **10** 183 (1974)
36. Töpfer J, Goodenough J B *J. Solid State Chem.* **130** 117 (1997)
37. Dabrowski B et al. *Phys. Rev. B* **58** 2716 (1998)
38. Dabrowski B et al. *Phys. Rev. B* **60** 7006 (1999)
39. Dabrowski B et al. *J. Solid State Chem.* **146** 448 (1999)
40. Bebenin N G, Zainullina R I, Ustinov V V *J. Magn. Magn. Mater.* **322** 963 (2010)
41. International Tables for Crystallography, http://it.iucr.org
42. Naish V E *Phys. Met. Metallogr.* **92** 317 (2001); *Fiz. Met. Metalloved.* **92** 3 (2001)
43. Kawano H et al. *Phys. Rev. B* **53** R14709 (1996)
44. Paraskevopoulos M et al. *J. Phys. Condens. Matter* **12** 3993 (2000)
45. Tomioka Y, Ito T, Sawa A *J. Phys. Soc. Jpn.* **84** 024703 (2015)
46. Rotiroti N et al. *Phys. Rev. B* **74** 104423 (2006)
47. Radaelli P G et al. *Phys. Rev. B* **56** 8265 (1997)
48. Beznosov A B et al. *Phys. Rev. B* **68** 054109 (2003)
49. Gaviko V S, Bebenin N G, Mukovskii Ya M *Phys. Rev. B* **77** 224105 (2008)
50. Kim K H et al., cond-mat/0212113
51. Biotteau G et al. *Phys. Rev. B* **64** 104421 (2001)
52. Rozenberg E et al. *Appl. Phys. Lett.* **92** 222506 (2008)
53. Zainullina R I et al. *Phys. Rev. B* **76** 014408 (2007)
54. Radaelli P G et al. *Phys. Rev. Lett.* **75** 4488 (1995)
55. De Teresa J M et al. *Phys. Rev. B* **54** 1187 (1996)
56. Aselage T L et al. *Phys. Rev. B* **68** 134448 (2003)
57. Huang Q et al. *Phys. Rev. B* **58** 2684 (1998)
58. Loa I et al. *Phys. Rev. Lett.* **87** 125501 (2001)
59. Pinsard-Gaudart L et al. *Phys. Rev. B* **64** 064426 (2001)
60. Neifeld E A et al. *J. Magn. Magn. Mater.* **295** 77 (2005)
61. Asamitsu A et al. *Phys. Rev. B* **54** 1716 (1996)
62. Laukhin V et al. *Phys. Rev. B* **63** 214417 (2001)
63. Arkhipov V E et al. *JETP Lett.* **71** 114 (2000); *Pis'ma Zh. Eksp. Teor. Fiz.* **71** 169 (2000)
64. Arkhipov V E et al. *Phys. Rev. B* **61** 11229 (2000)
65. Moritomo Y, Asamitsu A, Tokura Y *Phys. Rev. B* **51** 16491(R) (1995)
66. Laukhin V et al. *Phys. Rev. B* **63** 214417 (2001)
67. Neumeier J J et al. *Phys. Rev. B* **52** R7006 (1995)
68. Phan M H et al. *J. Alloys Compounds* **508** 238 (2010)
69. Shtrikman S, Wohlfarth E P *Physica* **60** 427 (1972)
70. Abdulvagidov Sh B et al. *JETP Lett.* **84** 31 (2006); *Pis'ma Zh. Eksp. Teor. Fiz.* **84** 33 (2006)
71. Sarkar P et al. *Phys. Rev. B* **78** 012415 (2008)
72. Rivadulla F, Rivas J, Goodenough J B *Phys. Rev. B* **70** 172410 (2004)
73. Banerjee B K *Phys. Lett.* **12** 16 (1964)
74. Bebenin N G et al *J. Magn. Magn. Mater.* **354** 76 (2014)
75. Shannon R D *Acta Cryst. A* **32** 751 (1976)
76. Mira J et al. *Phys. Rev. B* **65** 024418 (2001)
77. Koroleva L I et al. *JETP* **104** 76 (2007); *Zh. Eksp. Teor. Fiz.* **131** 85 (2007)
78. Kadomtseva A M et al. *Phys. Solid State* **42** 1110 (2000); *Fiz. Tverd. Tela* **42** 1077 (2000)
79. Tishin A M, Spichkin Y I *The Magnetocaloric Effect and its Applications* (Bristol: IOP Publ., 2003)
80. Gschneidner K A (Jr.), Pecharsky V K, Tsokol A O *Rep. Prog. Phys.* **68** 1479 (2005)
81. Phan M-H, Yu S-C *J. Magn. Magn. Mater.* **308** 325 (2007)
82. Kuz'min D, Richter M, Tishin A M *J. Magn. Magn. Mater.* **321** L1 (2009)
83. Bebenin N G, Zainullina R I, Ustinov V V *J. Appl. Phys.* **113** 073907 (2013)
84. Szymczak R et al. *J. Mater. Sci.* **43** 1734 (2008)
85. Okuda T et al. *Phys. Rev. Lett.* **81** 3203 (1998)
86. Okuda T et al. *Phys. Rev. B* **61** 8009 (2000)
87. Hamilton J J et al. *Phys. Rev. B* **54** 14926 (1996)
88. Lin P et al. *J. Appl. Phys.* **87** 5825 (2000)
89. Ziese M, Semmelhack H C, Busch P *J. Magn. Magn. Mater.* **246** 327 (2002)
90. Likodimos V, Pissas M *Phys. Rev. B* **73** 214417 (2006)
91. Markovich V et al. *Phys. Rev. B* **65** 144402 (2002)
92. Viglin N A, Naumov S V, Mukovskii Ya M *Phys. Solid State* **43** 1934 (2001); *Fiz. Tverd. Tela* **43** 1855 (2001)
93. Hazama H et al. *Phys. Rev. B* **62** 15012 (2000)
94. Golenishchev-Kutuzov A V et al. *Phys. Solid State* **57** 1633 (2015); *Fiz. Tverd. Tela* **57** 1596 (2015)
95. Darling T W et al. *Phys. Rev. B* **57** 5093 (1998)
96. Landau L D, Lifshitz E M *Theory of Elasticity* (Oxford: Pergamon Press, 1986); Translated from Russian: *Teoriya Uprugosti* (Moscow: Fizmatlit, 2003)
97. Zainullina R I et al. *Phys. Rev. B* **66** 064421 (2002)
98. Zainullina R I et al. *J. Alloys Compounds* **394** 39 (2005)
99. Zainullina R I, Bebenin N G, Ustinov V V, Shulyatev D A *Phys. Solid State* **59** 283 (2017); *Fiz. Tverd. Tela* **59** 275 (2017)
100. Zainullina R I et al. *J. Magn. Magn. Mater.* **300** e137 (2006)
101. Fertman E et al. *AIP Adv.* **5** 077189 (2015)
102. Belevtsev B I et al. *Phys. Rev. B* **74** 054427 (2006)
103. Landau L D, Lifshitz E M *Statistical Physics* Vol. 1 (Oxford: Pergamon Press, 1980); Translated from Russian: *Statisticheskaya Fizika* Ch. 1 (Moscow: Fizmatlit, 2002)
104. Iliev M N et al. *Phys. Rev. B* **57** 2872 (1998)
105. Wdowik U D, Koza M M, Chatterji T *Phys. Rev. B* **86** 174305 (2012)
106. Fedorov I et al. *Phys. Rev. B* **60** 11875 (1999)
107. Mostovshchikova E V *Sol. State Commun.* **150** 1884 (2010)
108. Hennion M, Moussa F *New J. Phys.* **7** 84 (2005)
109. Reichardt W, Braden M *Physica B* **263** 416 (1999)
110. Endoh Y, Hirota K *J. Phys. Soc. Jpn.* **66** 2264 (1997)
111. Vasiliu-Doloc L et al. *J. Appl. Phys.* **83** 7342 (1998)
112. Adams C P et al. *Phys. Rev. B* **70** 134414 (2004)
113. Ye F et al. *Phys. Rev. B* **75** 144408 (2007)
114. Moussa F et al. *Phys. Rev. B* **76** 064403 (2007)
115. Tapan T, Regnault L P, Schmidt W *Phys. Rev. B* **66** 214408 (2002)
116. Arsenov A A et al. *Phys. Status Solidi A* **189** 673 (2002)
117. Lofland S E et al. *Phys. Lett. A* **233** 476 (1997)
118. Lofland S E et al. *Phys. Rev. B* **56** 13705 (1997)
119. Ivannikov D et al. *Phys. Rev. B* **65** 214422 (2002)
120. Deisenhofer J et al. *Phys. Rev. Lett.* **95** 257202 (2005)
121. Eremina R M et al. *JETP Lett.* **85** 51 (2007); *Pis'ma Zh. Eksp. Teor. Fiz.* **85** 57 (2007)
122. Yatsik I V et al. *JETP Lett.* **87** 447 (2008); *Pis'ma Zh. Eksp. Teor. Fiz.* **87** 517 (2008)
123. Auslender M et al. *J. Appl. Phys.* **109** 07D705 (2011)
124. Auslender M et al. *J. Appl. Phys.* **113** 17D705 (2013)
125. Mikhalev K N, Volkova Z N, Gerashchenko A P *Phys. Met. Metallogr.* **115** 1139 (2014); *Fiz. Met. Metalloved.* **115** 1204 (2014)
126. Pickett W E, Singh D J *Phys. Rev. B* **53** 1146 (1996)
127. Pickett W E, Singh D J *J. Magn. Magn. Mater.* **172** 237 (1997)
128. Papaconstantopoulos D A, Pickett W E *Phys. Rev. B* **57** 12751 (1998)

129. Loshkareva N N et al. *JETP* **94** 350 (2002); *Zh. Eksp. Teor. Fiz.* **121** 412 (2002)
130. Krivoruchko V N, D'yachenko A I, Tarenkov V Yu *Low Temp. Phys.* **39** 211 (2013); *Fiz. Nizk. Temp.* **39** 276 (2013)
131. Livesay E A et al. *J. Phys. Condens. Matter* **11** L279 (1999)
132. Hamid A S, Arima T *Phys. Status Solidi B* **241** 345 (2004)
133. Korotin M, Fujiwara T, Anisimov V *Phys. Rev. B* **62** 5696 (2000)
134. Auslender M, Kogan E *Eur. Phys. J. B* **19** 525 (2001)
135. Nagaev E L *Physics of Magnetic Semiconductors* (Moscow: Mir Publ., 1983); Translated from Russian: *Fizika Magnitnykh Poluprovodnikov* (Moscow: Nauka, 1979)
136. Bebenin N G et al. *J. Phys. Condens. Matter* **17** 5433 (2005)
137. Bebenin N G et al. *JETP* **90** 1027 (2000); *Zh. Eksp. Teor. Fiz.* **117** 1181 (2000)
138. Bebenin N G et al. *Phys. Met. Metallogr.* **103** 261 (2007); *Fiz. Met. Metalloved.* **103** 271 (2007)
139. Bebenin N G et al. *Phys. Met. Metallogr.* **108** 232 (2009); *Fiz. Met. Metalloved.* **108** 243 (2009)
140. Bebenin N G et al. *Phys. Rev. B* **78** 064415 (2008)
141. Alexander S, Helman J S, Balberg I *Phys. Rev. B* **13** 304 (1976)
142. Vonsovskii S V *Magnetism* (New York: Wiley, 1974); Translated from Russian: *Magnetizm* (Moscow: Nauka, 1971)
143. Asamitsu A, Tokura Y *Phys. Rev. B* **58** 47 (1998)
144. Bebenin N G et al. *Phys. Rev. B* **69** 104434 (2004)
145. Lyanda-Geller Y et al. *Phys. Rev. B* **63** 184426 (2001)
146. Bebenin N G et al. *J. Phys. Condens. Matter* **17** 5433 (2005)
147. Chun S H, Salamon M B, Han P D *Phys. Rev. B* **59** 11155 (1999)
148. Kuwahara H et al. *J. Appl. Phys.* **93** 7367 (2003)
149. Hurd C M *The Hall Effect in Metals and Alloys* (New York: Plenum Press, 1972)
150. Vedyaev A V, Granovskii A B, Kotel'nikova O A *Kineticheskie Yavleniya v Neuporyadochennykh Ferromagnitnykh Splavakh* (Kinetic Phenomena in Disordered Ferromagnetic Alloys) (Moscow: Izd. MGU, 1992)
151. Mott N F, Davis E A *Electronic Processes in Non-Crystalline Materials* (Oxford: Clarendon Press, 1979); Translated into Russian: *Elektronnye Protsessy v Nekristallicheskikh Veshchestvakh* (Moscow: Mir, 1982)
152. Asamitsu A, Moritomo Y, Tokura Y *Phys. Rev. B* **53** R2952 (1996)
153. Uhlenbruck S et al. *Phys. Rev. B* **57** R5571 (1998)
154. Zainullina R I et al. *Phys. Solid State* **45** 1754 (2003); *Fiz. Tved. Tela* **45** 1671 (2003)
155. Jaime M et al. *Phys. Rev. B* **60** 1028 (1999)
156. Zvyagin I P "The hopping thermopower", in *Hopping Transport in Solids* (Amsterdam: North-Holland, 1991)
157. Zhou J-S, Goodenough J B *Phys. Rev. B* **64** 024421 (2001)
158. Fujishiro H, Ikebe M *AIP Conf. Proc.* **554** 433 (2001)
159. Okimoto Y et al. *Phys. Rev. B* **55** 4206 (1997)
160. Takenaka K et al. *Phys. Status Solidi B* **215** 637 (1999)
161. Nomerovannaya L V, Makhnev A A, Rumyantsev A Yu *Phys. Solid State* **41** 1322 (1999); *Fiz. Tverd. Tela* **41** 1445 (1999)
162. Nomerovannaya L V, Makhnev A A , Rumyantsev A Yu *Phys. Met. Metallogr.* **89** 258 (2000); *Fiz. Met. Metalloved.* **89** 51 (2000)
163. Takenaka K, Shiozaki R, Sugai S *Phys. Rev. B* **65** 184436 (2002)
164. Bebenin N G et al. *J. Phys. Condens. Matter* **22** 096003 (2010)
165. Rauer R, Rübhausen M, Dörr K *Phys. Rev. B* **73** 092402 (2006)
166. Sukhorukov Yu P et al. *J. Appl. Phys.* **91** 4403 (2002)
167. Telegin A V et al. *J. Magn. Magn. Mater.* **383** 104 (2015)
168. Mostovshchikova E V, Bebenin N G, Loshkareva N N *Phys. Rev. B* **70** 012406 (2004)
169. Mostovshchikova E V *Solid State Commun.* **150** 1884 (2010)
170. Samokhvalov A A , Tutikov N M, Skornyakov G P *Fiz. Tverd. Tela* **10** 2760 (1986)
171. Gerthsen P et al. *Solid. State Commun.* **3** 165 (1965)
172. Arbuzova T I, Naumov S V, Bebenin N G *JETP Lett.* **98** 80 (2013); *Pis'ma Zh. Eksp. Teor. Fiz.* **98** 88 (2013)
173. Arbuzova T I, Naumov S V *JETP Lett.* **101** 760 (2015); *Pis'ma Zh. Eksp. Teor. Fiz.* **101** 857 (2015)